Summer 2011

Bond strength of high-volume fly ash concrete

Michael Hayse Wolfe

Department:

BOND STRENGTH OF HIGH-VOLUME FLY ASH CONCRETE

by

MICHAEL HAYSE WOLFE

A THESIS

Presented to the Faculty of the Graduate School of the

MISSOURI UNIVERSITY OF SCIENCE AND TECHNOLOGY

In Partial Fulfillment of the Requirements for the Degree

MASTER OF SCIENCE IN CIVIL ENGINEERING

2011

Approved by

Dr. Jeffrey Volz, Advisor
Dr. John Myers
Dr. David Richardson

ABSTRACT

Concrete is the most consumed man-made material in the world. Unfortunately, due to the production of cement, concrete has a large carbon footprint. Replacement of cement with fly ash, an industrial waste product, offers a sustainable alternative. The goal of this research was to explore the feasibility of using high-volume fly ash (HVFA) concrete for structural applications by testing the material's reinforcement bond properties.

A series of pull-out tests and beam splice tests were performed on specimens with a 70 percent fly ash replacement of cement and then compared to identical tests performed on control specimens cast from a 100 percent portland cement mix. The pull-out tests were performed on specimens with either No. 4 or No. 6 bars, while the beam splice tests were performed on specimens with No. 6 bars with and without confinement (transverse reinforcement) along the splice zone.

The data recorded from the pull-out tests supports the effectiveness of HVFA concrete in terms of bond integrity. Since the pull-out test is a comparative test, this conclusion can be drawn based on the fact that the HVFA specimens demonstrated similar bond strengths to the control specimens (based on maximum modified applied load). The only drawback from testing was that once the concrete began to crush around the reinforcing bar, slip occurred at a higher rate for the HVFA specimens.

The load data collected from the splice tests, once modified for the respective specimen compressive strengths, indicates that the HVFA concrete specimens were able to support more load than the control specimens before the splice failed. These findings, along with the findings from the pull-out tests, indicate that the use of high volumes of fly ash as a cement substitute is not only feasible in terms of bond, but also superior in some cases.

.

ACKNOWLEDGMENTS

First and foremost, I would like to thank my advisor, Dr. Jeffrey Volz for being an amazing mentor throughout the research and writing phases of my degree. Without his guidance and friendship, none of this would have been possible.

I would like to thank Ameren UE, Mississippi Lime, USA gypsum, and BASF for supplying the funding and materials necessary to complete this project.

I would also like to thank the members of my committee, Dr. Dave Richardson and Dr. John Myers for reviewing my thesis and making important suggestions that greatly added to the quality of the final product.

I would like to thank Mike Lusher. Without his enthusiasm and great knowledge of the various test methods and laboratory equipment, my research would not have run nearly as smoothly as it did. I will truly miss working in the same office as him. I will always consider him a mentor and friend.

I would like to thank Gary Abbot, Steve Gabel, John Bullok, Jason Cox, Mark Ezzell, Carlos Ortega, Kyle Marlay, Krista Porterfield, and Marc Mastrantuono for their hard work while helping me with the construction and testing phases of my specimens.

I would also like to thank my roommates, Ryan Haney, Bret Grinde, and Ryan Stringer, as well as the many friends that I have made during my stay in Rolla. They have made my college experience an amazing one and I hope to keep in contact with them after graduation.

Last but not least, I would like to thank my parents, Greg and Cindy Wolfe, and my grandparents, Don and Joan Wolfe, for supporting me throughout my life. They have really been the driving force behind me advancing this far in my education and life. I seriously doubt I would have been able to get this far without their love and guidance.

TABLE OF CONTENTS

Page

LIST OF FIGURES

LIST OF TABLES

1. INTRODUCTION

1.1. BACKGROUND

1.1.1. General. Fly ash is a mineral waste product of the coal burning process used in many power plants around the world. Currently, only about 25 to 30 percent of this material is recycled and used as a mineral admixture in concrete and in other applications, such as soil stabilization. The rest, about 70 to 75 percent is typically buried in landfills (Coal Fly Ash – Material Description, 2010). The two most common classes of fly ash used in concrete are Class C and Class F. Both classes are pozzolanic, meaning they react with excess calcium hydroxide (CH) in concrete, formed from cement hydration, to form calcium silicate hydrate (CSH), but the Class C also contains higher levels of calcium. This calcium content gives the Class C fly ash a self-setting quality when it comes in contact with water (Coal Fly Ash – Material Description, 2010).

1.1.2. Benefits of Fly Ash in Concrete. Research shows that adding fly ash to concrete, as a partial replacement of cement (less than 35 percent), will benefit both the fresh and hardened states. While in the fresh state, the fly ash improves workability. This is due to the smooth, spherical shape of the fly ash particle. The tiny spheres act as a form of ball bearing that aids the flow of the concrete (Morotta, 2005). This improved workability allows for lower water-to-cement ratios, which later leads to higher compressive strengths (Mindess, et al., 2003). In the hardened state, fly ash contributes in a number of ways, including strength and durability. While fly ash tends to increase the setting time of the concrete, the 28 day strengths tend to be higher than those of conventional concretes. This is due to the pozzolanic reaction removing the excess calcium hydroxide, produced by the cement reaction, and forming a harder CSH

(Headwaters Resources, Fly Ash for Concrete). Another improved hardened state property is bond strength. The inclusion of fly ash in concrete causes most pastes to become denser due to increased amounts of CSH as well as lower water to cement ratios. This increase in paste volume allows the paste to fill in more of the gaps around the reinforcing bars, increasing the surface are of the bond, and leading to higher bond strengths (ACI Committee 232, 2003). In addition, the denser paste produced from fly ash improves permeability by filling in voids, making the concrete more durable. A benefit of lower permeability is that chlorides are prevented from diffusing into the concrete and corroding the rebar (Headwaters Resources, Fly Ash for Concrete).

1.1.3. High-Volume Fly Ash Concrete. Substituting higher amounts of portland cement with fly ash allows for more fly ash to be recycled instead of buried in a landfill. The current ACI recommendation for fly ash substitution in concrete is 15-35 percent (ACI Committee 232, 2003). High-volume fly ash (HVFA) concrete is defined by ACI as having a fly ash substitution of 50 percent or more (ACI Committee 232, 2003). Using this excess fly ash for concrete benefits the environment and possibly concrete integrity.

1.1.3.1. Environmental benefits. According to a study done in 2009, seven percent of green house emissions in 2004 were due to the manufacture of cement (Berry, et al., 2009). These emissions are due to the carbon dioxide produced from machinery mining virgin material, transporting the material to cement plants, and from the kiln used to burn these materials in order to make the actual cement (Hanle et al., 2004). According to Bargaheiser and Butalia, one ton of carbon dioxide gas is emitted per one ton of portland cement manufactured (Bargaheiser and Bualia, n.d.). Since fly ash is a byproduct of burning coal, a necessary process that will continue for years to come, and

cement is a carbon dioxide emitting process involving virgin materials, using larger amounts of fly ash in concrete could possibly decrease the amount of green house gasses emitted from cement production by half as the demand for cement decreases.

1.1.3.2. Setbacks. The main setback with using high-volume fly ash concrete in construction is the increased setting time. Retarded set time delays form removal, which increases time of construction (Morotta, 2005). Since labor is the primary cost contributing factor in construction, the setting time of high-volume fly ash concrete must be accelerated. One method of acceleration is adding lime (calcium hydroxide) to the mix. The addition of lime supplies the fly ash with the calcium hydroxide necessary for the pozzolanic reaction to start earlier. Research performed at the National Institute of Standards and Technology indicates that the addition of CH to high-volume fly ash concrete provides a significant boost to setting time (Bentz and Ferraris, 2009)

1.2. OBJECTIVE AND SCOPE OF WORK

Currently, high-volume fly ash (HVFA) concrete is used mostly for ornamentation and various non load bearing applications. Few structures have been built utilizing this less proven material. The ***objective*** of this study was to explore the effects of substituting large amounts of fly ash on the concrete to reinforcement bond strength, which, ultimately, along with other strength and durability tests, examined the feasibility of using HVFA concrete for the sustained construction of structures.

As a means of testing the bond strength of HVFA concrete, the following scope of work was developed and followed:

- Perform a literature review;

- Develop mix designs for both control and HVFA concrete;
- Design and construct test fixtures;
- Design and construct pull-out and splice specimens;
- Test specimens to failure;
- Record and analyze data from tests; and
- Develop conclusions and recommendations.

1.3. RESEARCH PLAN

In order to carry out the scope of work for this project, a set of tasks, or benchmarks, was established. These tasks are as follows:

Task 1: Perform a literature review. The goal of the literature review is to become familiarized with testing methods and results from previous research. This knowledge can be used to better understand the behavior of the specimens, avoid mistakes, as well as provide a source with which to compare test results to support plausibility.

Task 2: Develop experimental and control mix designs. In order to achieve the desired early strengths for HVFA concrete, a mix design utilizing the optimal percentage of fly ash, calcium hydroxide (CH), and gypsum must be designed. Also important will be to design a similar 100 percent portland cement control mix with which to test against the HVFA concrete mix design. Both mixes will be decided upon by a series of mortar cube and concrete cylinder compressive strength tests. The compression tests will be performed at 1, 2, 14, and 28 days for all cube and cylinder types.

Task 3: Perform tensile tests on 3/4-inch-diameter (19 mm) reinforcing bar. The test specimens for this task will be the same type of reinforcement used in the splice test. Relevant data from these tests will indicate the strain present in the bars when yielding occurs. The recorded yield strains will then be used to confirm the failure mode based on the measured strains in the bars within the splice tests.

Task 4: Develop formwork and test fixtures. In order to mold the concrete to the shape and dimensions needed for both the pull-out and splice specimens, a series of forms must be constructed to accommodate the necessary steel and concrete. Also important are the fixtures that will be applying the loads necessary to test the specimens.

Task 5: Analyze recorded test data. After testing the specimens constructed as a part of Task 4, the data will need to be organized in such a way that conclusions can be drawn. Hence, a series of tables and plots will be formed to meet this goal.

1.4. OUTLINE

This thesis is comprised of six sections, as well as three appendices. Information regarding the sections and appendices can be found below.

Section 1 acts as an introduction to the thesis. This introduction contains a brief background of fly ash as a material, fly ash as an additive to concrete, and the environmental concerns regarding cement production. Also available is the scope of work as well as an order of operations for the tasks required for this study.

Section 2 is the literature review portion of this study. Information regarding past research on bond testing of HVFA as well as bond testing in general can be found in this section.

Chapter 3 contains a report regarding the preliminary material testing and results necessary to design a mix suitable for testing. Also available in this section are the results for the steel tensile testing.

Section 4 includes the specimen fabrication, test procedure, results, and discussion for the pull-out tests performed as a part of this study.

Section 5 includes the specimen fabrication, test procedure, results, and discussion for the beam splice tests performed as a part of this study.

Section 6 contains a summary of the conclusions drawn from this study as well as suggestions for future research.

There are three appendices. Appendix A contains data tables from the pull-out and beam splice tests, Appendix B contains plots from the pull-out and beam splice tests, and Appendix C contains tables and plots related to the mix development stage of this study. Appendix D contains a statistical analysis (t-test) of the averaged data for both the pull-out tests and the beam splice tests.

2. LITERATURE REVIEW

2.1. CONCRETE BOND

Concrete, on its own, is strong in compression but weak in tension. As a matter of fact, the compressive strength of concrete is about ten times greater than its tensile strength. This negative trait is remedied by placing steel reinforcing bars into the concrete to form reinforced concrete (RC). This approach allows a material with much higher tensile strength, such as steel, to take on the tensile load that the concrete cannot support. In order for this relationship to work, however, the concrete and the reinforcing steel must have a sufficient bond between them so the tensile load can be transferred effectively to the steel. There are three different aspects that contribute to bond strength: chemical adhesion, friction, and mechanical interlock. The chemical adhesion is a bond between the concrete and the steel, the friction is caused by the bar deformations, or ribs, slipping along the concrete, and the mechanical interlock is a bearing force caused by the ribs bearing against the concrete (Swenty, 2003).

In order to insure an adequate bond, ACI 318 (2008) regulates how long a bar must be imbedded into the concrete based on factors such as concrete type, concrete strength, bar diameter, and bar type. This regulated factor is called the development length of the bar, and prevents a bond failure from being the controlling failure mode of a structure.

Bond failure usually occurs in two different ways. In structures, the most common is known as a splitting failure. A splitting failure occurs when a small clear cover or small spacing between reinforcing bars exists. The small amount of concrete

around the bars can crack or split, exposing the reinforcement and ultimately leading to bond failure. Also contributing to a splitting failure are the mechanical properties of the surrounding concrete such as concrete tensile strength, bar geometry, and the presence of transverse reinforcement such as stirrups (ACI Committee 408, 2003). This result tends to be the more catastrophic of the bond failure modes (Swenty, 2003). Another common bond failure type is pull-out. This mode occurs when the reinforcing bar slips, and as a result, the concrete between the bar deformations is crushed, leading to a simple pulling out of the bar. Usually pull-out controls when there is a larger concrete clear cover and spacing between the reinforcing bars making splitting less likely. A less common bond failure is known as a conical failure. This occurs when the concrete cracks propagate outward from the ribs on a reinforcing bar, and the bar ultimately pulls out along with a "cone" of concrete upon failure.

2.2. BOND TESTING

Testing for bond strength is carried out in a variety of ways. The most common and traditional method is the standard pull-out test. One issue with the pull-out test is that a compressive stress is induced on the bond that normally does not exist in an actual structure. To remedy this, ACI 408R-03 outlines several other methods such as the beam anchorage, beam end, and splice tests that place the bond in situations that are more similar to those present in the field (ACI Committee 408, 2003). Note that the following ACI bond tests do not have specimen dimensions. This is because ACI does not specify specific dimensions.

The pull-out test is popular due to its ease of construction and testing. ASTM C234 was developed to standardize the testing method, but was later disbanded due to the high level of inconsistency that the test yields. RILEM, however, has provided a set of recommendations for the test in order to provide some form of uniformity and minimize some of the inconsistencies. The RILEM test recommends casting a single reinforcing bar into a concrete cube with only half of the bar inside the specimen actually bonded to the concrete, as shown in **Figure 2.1** (RILEM 7-II-28, 1994). This approach is to prevent a conical bond failure at the bottom and is achieved using a bond breaker of some type. The bar is fed through a metal plate and a pulling force is applied to the bar while the metal plate pushes up on the concrete block until a bond failure occurs. Usually a device is installed on the unloaded end of the reinforcing bar in order to measure slip. While this test has been modified by RILEM, it is still not accepted as an accurate way of determining development lengths for reinforcement (ACI Committee 408, 2003). Therefore, this test is commonly used as a means of comparison between a control specimen of known development requirements and an experimental specimen. Data for this test is often compiled into force vs. slip and stress vs. slip plots.

The beam anchorage test, a large scale test, involves casting a beam with two points of exposed rebar located on the bottom of the beam, to either side of the center, as shown in **Figure 2.2**. These two points represent flexural cracks in the beam. Knowing the bonded length of the reinforcement is also important. Once cast and cured, the beam is then subjected to a four-point loading until failure occurs (ACI Committee 408, 2003).

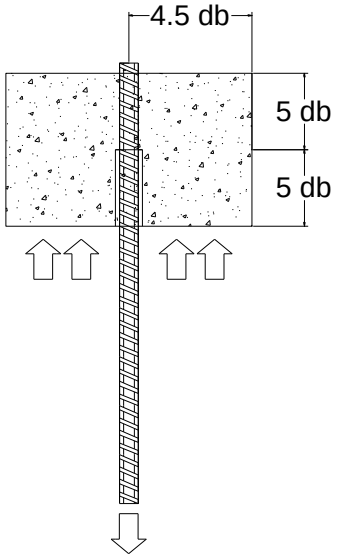

Figure 2.1 – Typical pull-out specimen (d_b = bar diameter)

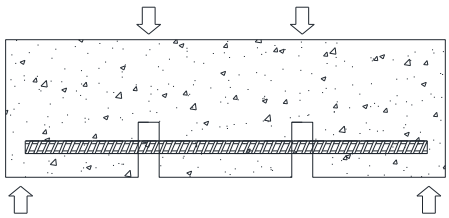

Figure 2.2 – Beam anchorage specimen (ACI 408R-03)

The beam end test was also developed to provide a more accurate means of testing bond strength. This test is very similar to the pull-out test, except the reactions, or supports, are set up in a way that does not cause compression around the single reinforcing bar. In this case, the reinforcing bar is cast near the top of the concrete block,

also with a bond breaker, and a pulling force is applied to the bar (ACI Committee 408, 2003). **Figure 2.3** outlines the support setup as well as the general specimen setup.

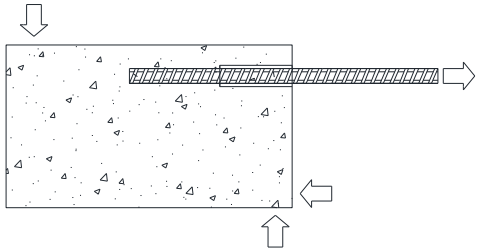

Figure 2.3 – Beam end specimen (ACI 408R-03)

Another form of large scale bond testing is the splice test. The splice test involves casting spliced reinforcing bars into a beam and applying a four-point loading, as shown in **Figure 2.4**. The splice test can be run with or without transverse reinforcement along the spliced area. This test, due to a more accurate representation of structural conditions, was used to gather the majority of the data that was used in the formulation of the development length and splice length equations in the ACI 318 code (ACI Committee 408, 2003).

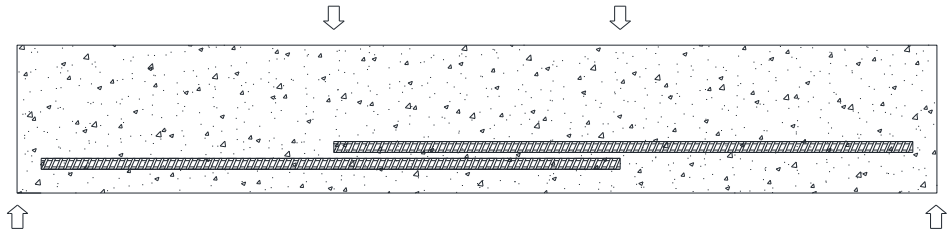

Figure 2.4 – Splice specimen (ACI 408R-03)

In 2000, two researchers, Zuo and Darwin, ran multiple splice tests on specimens composed of normal strength concrete and high strength concrete. The beams had a height of either 15.5 (394 mm) or 16 in. (406 mm), a width of either 12 (305 mm) or 18 in. (457 mm), and a length of 16 feet (4877 mm). Each beam contained either two or three splices which ranged in length from 16 (406 mm) to 40 in. (1016 mm). These splices were cast into the upper region of the beam with a 2 in. (51 mm) concrete cover. Also varied in this experiment was the presence of transverse reinforcement along the splices. The beams were supported 3 feet to either side of the center and were tested in a cantilever manner at each end. Several observations were made after the failure of each beam. First, it was observed that each beam failed due to a splitting failure caused by the failure of the splice itself. Second, the high strength concrete failed at a higher load, which supports the theory that higher concrete compressive strengths positively affect bond strength. Finally, the concrete without the transverse reinforcement along the splice failed more suddenly than the beams containing the transverse reinforcement (Zuo and Darwin, 2000).

Splice testing was also performed by Russell and Ramirez (2008) to examine the effects of high strength concrete on bond. The specimens were similar to the full size beams used by Zuo and Darwin (2000), except strain gages were installed on either side of the splices as well as 9 in. (229 mm) to either side of each splice. The strain gages were utilized to observe the strain behavior of the steel as the specimen was loaded. Other factors tested were the effects of bar size (testing Nos. 6, 8, and 10 bars (19, 25, and 32 mm bars) and confinement. All beams contained three spliced bars that were cast into the upper portion of each concrete beam (with at least 12 in. (305 mm) of concrete

cast below the splice). The beams had a length of 13 ft. (3962 mm) and a cross section (width x height) of 9 x 18 in. (229 x 457 mm), 12 x 18 in. (305 x 457 mm), and 18 x 18 in. (457 x 457 mm) for the Nos. 6, 8, and 10 bars (19, 25, and 32 mm bars), respectively. The minimum concrete compressive strength for this experiment was 15 ksi (103 MPa). The specimens were supported 2 ft. (610 mm) to either side of the center and were tested in a cantilever manner at each end. Each beam, when tested, failed at the splice. The results from this study show that both the larger bar sizes and confinement add to the bond strength of concrete (Russell and Ramirez, 2008).

2.3. HIGH-VOLUME FLY ASH BOND RESEARCH

While the concept of replacing a large percentage of portland cement with fly ash is a fairly new idea, several research programs have explored the bond between high-volume fly ash concrete and the reinforcing steel. These programs commonly used a standard pull-out test with varying percentages of fly ash.

Researchers at Montana State University ran a series of pull-out tests on high-volume fly ash specimens utilizing one hundred percent replacement of portland cement. This high percentage replacement was possible due to the highly reactive nature of the Class C fly ash used. The specimen design involved a No. 4 (No. 13) bar embedded into a concrete cylinder with a diameter of 6 in. (152 mm) and a height of 12.3 in. (312 mm). The embedment depth was varied so that three bars were embedded 8 in. (203 mm) and three others to 12 in. (305 mm) for each material. No bond breaker was used nor was any rebar exposed on the unloaded end for the measuring of slip. Six control specimens made from normal portland cement concrete were tested at the two different embedment depths

(three at 8 in. (203 mm) and three at 12 in. (305 mm)) along with six high-volume fly ash specimens with the same two embedment depths. The results were then recorded and compared. The results were very similar between the normal concrete and the high-volume fly ash concrete, with all specimens failing due to splitting (Cross, et al., n.d.). This type of bond failure might have been due to a small clear cover coupled with the large bar size.

Researchers at the University of Wisconsin-Milwaukee performed pull-out tests on specimens with fly ash replacements of 10, 20, and 30 percent. Also varied with the fly ash content was the temperature at which the specimens were cured. These tests were run on typical pull-out specimens as suggested by RILEM and ACI. For each specimen, a single piece of reinforcing bar was set vertically into a concrete cylinder with a radius of six in. and a height of six in. A specimen was made for each temperature condition and percentage of specimen. The bar was then pulled out of the cylinder at a rate of 0.081 in. (2 mm) per minute. Once the data was recorded and analyzed, a trend became apparent. At normal temperature, the bond strength improved with the increase in fly ash, up until a point. At this point, about 20 percent fly ash, the bond strengths began to decrease (Naik, et al., 1989). While none of these specimens can be classified as a high-volume fly ash concrete specimen, according to ACI's definition (50 percent replacement), these series of tests at varying fly ash percentages give insight to how bond strength is affected at different intervals. This result could lead to an understanding of how bond behaves in high-volume fly ash concrete.

Pull-out specimens were also tested at the Structural Engineering Research Centre in India to determine the effects on bond strength using a 50 percent fly ash replacement

of cement. A typical specimen was composed of a single, 0.79 inch (20 mm) steel reinforcement rod embedded into a 5.9 inch (150 mm) concrete cube. Specimens tested at 28 days yielded similar results between the high-volume fly ash concrete and the control concrete, with the control concrete having a slight edge. The high-volume fly ash concrete, however, surpassed the control specimens in bond strength at 90 days (S. Gopalakrishnan, 2005).

2.4. INDICATORS FOR FLY ASH EFFECTS ON BOND

The effects of fly ash on concrete bond strength can be seen through experimentation, but there are also several properties that contribute to the bond strength of normal concrete that could provide insight to how high-volume fly ash concrete might behave in relation to bond. These properties can be used as predictors, one of which is the tensile strength of concrete, obtained by the split cylinder test. According to ACI 408R, bond is directly affected by concrete tensile strength (ACI Committee 408, 2003). This would explain why a splitting failure is the most common bond failure in structures (ACI Committee 408, 2003). Therefore, if the high-volume fly ash concrete's results are lower for the split cylinder test, the bond could possibly be adversely affected as well. The same trend may apply to compressive strength of the concrete as well. If the high-volume fly ash concrete has a lower compressive strength, then according to trends, it will also have lower bond strength. ACI 232.2R (2003) theorizes that if a high-volume fly ash concrete has a similar compressive strength to that of a normal concrete, then the

two should have the same reinforcement development length. Also, due to the tendency of fly ash to increase paste volume, the contact area between the paste and the reinforcement tends to increase, improving bond strength (ACI Committee 232, 2003).

3. MIX DESIGN

3.1. INTRODUCTION

This section describes the process that was carried out to develop a concrete mix design using a high volume of cement replacement with fly ash. The objective of this process was to maximize the percentage of fly ash in the mix, yet still fulfill the strength and workability requirements. A target strength of 5,000 psi at 28 days was selected to perform the mix development based on the ACI 211.1, Standard Practice for Selecting Proportions for Normal, Heavyweight and Mass Concrete (ACI 211.1, 1991) document. Class C fly ash donated by Ameren UE was used as replacement of the portland cement due to its high level of calcium. This part of the study used mortar and paste mixes to arrive at the optimum combinations and percentages of several powder additions to maximize the amount of fly ash. The primary criteria to select such percentages were the set time and the rate of strength gain. The main goal was to develop a mix that could fulfill a minimum strength requirement of 1,000 psi at 1 day in addition to the requisite 5,000 psi at 28 days. Attainment of this goal would prove that the use of HVFA concrete in construction is viable. Rheological composition of the fly ash, mix design development, and compressive strength results are contained in the following sections.

3.2. FLY ASH CHEMICAL COMPOSITION

Fly ashes are subdivided into two main classes, C and F, which reflect the composition of the inorganic fractions. Class F fly ashes are produced from either anthracite bituminous or sub-bituminous coals. Class C fly ashes are derived from sub-

bituminous or lignitic coals. In other words, the two classes of fly ash are distinguished by the silica oxide and calcium contents of the type of coal burned. Fly ash can be cementitious, pozzolanic, or both. Class F fly ash is pozzolanic while Class C fly ash is often cementitious and pozzolanic. Cementitious fly ash hardens when wetted while pozzolanic fly ash requires a reaction with lime before hardening. Both classes of fly ash are used as a cement replacement in concrete.

The fly ash used in this study was an ASTM Class C fly ash produced in the coal-fired electrical generating plant of Ameren UE located in Labadie, Missouri. The chemical composition of the fly ash is given below in **Table 3.1**. Four samples of fly ash were tested for chemical composition. The amount of each oxide represents the range of the four samples expressed as a percent by weight. **Table 3.2** shows the typical ranges of the chemical composition of a Class C fly ash. The chemical oxide quantities reported in **Table 3.1** coincide with those listed in **Table 3.2**. All requirements are also in accordance with ASTM C618, Standard Specification for Coal Fly Ash and Raw or Calcined Natural Pozzolan for Use in Concrete (ASTM C618, 2007).

3.3. ACTIVATORS

Although certain fly ashes exhibit some cementitious properties, the main contribution to the hardened concrete properties results from the pozzolanic reaction of the fly ash with the calcium hydroxide released by the portland cement. The pozzolanic reaction typically occurs more slowly than cement hydration reactions and consequently concrete containing fly ash requires more curing during early ages. Previous research has shown that fly ash has very little immediate chemical reaction when it is only mixed with

water. There are enough oxides and aluminates within the portland cement to provide sufficient reaction in the process of hydration, whereas, fly ash requires the addition of activators to initiate the hydration process. The activators used in the HVFA concrete for this study were calcium hydroxide and gypsum, selected based on previous research. Appropriate proportions were determined to ensure a proper hydration process. Insufficient amounts of activators may generate a delay in reaching adequate early-age strengths. Excess amounts of activators may generate a rapid set or false set that may not develop the required densification of the microstructure, also affecting the concrete strength.

Table 3.1 – In-house chemical analysis of Ameren UE fly ash

Oxide	*%*
Silicon Oxide (SiO_2)	30.45 – 36.42
Aluminum Oxide (Al_2O_3)	16.4 – 20.79
Iron Oxide (Fe_2O_3)	6.78 – 7.73
Calcium Oxide (CaO)	24.29 – 26.10
Magnesium Oxide (MgO)	4.87 – 5.53
Sulfur (SO_3)	2.18 – 6.36
Sodium Oxide (Na_2O)	1.54 – 1.98
Potassium Oxide (K_2O)	0.38 – 0.57
Titanium Oxide (TiO_2)	1.42 – 1.56
Phosphorus Oxide (P_2O_5)	1.01 – 1.93
Manganese Oxide (MnO)	0.028 – 0.036
Strontium Oxide (SrO)	0.40 – 0.44
Barium Oxide (BaO)	0.68 – 0.99
LOI	0.24 – 1.15

Table 3.2 – Fly ash chemical differences expressed as percent by weight (ASTM C618-07)

Component	Bituminous	Sub-bituminous	Lignite
SiO_2	20 – 60	40 – 60	15 – 45
Al_2O_3	5 – 35	20 – 30	10 – 25
Fe_2O_3	10 – 40	4 – 10	4 – 15
CaO	1 – 12	5 – 30	15 – 40
MgO	0 – 5	1 – 6	3 – 10
SO_3	0 – 4	0 – 2	0 – 10
Na_2O	0 – 4	0 – 2	0 – 6
K_2O	0 – 3	0 – 4	0 – 4
LOI	0 – 15	0 – 3	0 – 5

3.3.1. Gypsum. Calcium sulfate dihydrate (gypsum) is added to portland cement to limit the vigorous initial reaction of the tricalcium aluminate (C_3A) with water, which can lead to a flash set. However, fly ash has a slower initial setting time. When fly ash is used in large amounts, such as in a HVFA concrete consisting of 70 percent fly ash replacement, additional gypsum may be required to prevent sulfate depletion and promote the immediate start of the hydration process.

The gypsum used in this study was obtained from the company USA Gypsum located in Reinholds, PA, where it is produced from recycled gypsum boards. Gypsum board, otherwise known as dry wall, is regularly used as a building interior lining and partitioning where structural requirements are low. The panels of dry wall are made of gypsum plaster pressed between two thick sheets of paper. The gypsum used in this study was ground to an ultra-fine consistency with a 96% pure content of calcium sulfate ($CaSO_4$). **Figure 3.1** shows the packaging and gypsum material used in this study.

Figure 3.1 – Gypsum material sample

The mixture proportion for gypsum was determined from a previous study carried out by Bentz [2010]. Bentz studied a 50:50 ratio of portland cement to fly ash, and found that at least 2 percent additional gypsum by mass of total cementitious materials was required for a proper hydration. Having a higher fly ash content would likely require more than two percent of gypsum, so it was decided to use a 4 percent replacement of the fly ash with gypsum. This amount proved to be effective in testing of paste and mortar cubes, the results of which will be discussed later in this section.

3.3.2. Calcium Hydroxide. In conventional concrete, the tricalcium silicate (C_3S) and dicalcium silicate (C_2S) react individually with water to produce the principal hydration product of calcium silicate hydrate (C-S-H) and calcium hydroxide (CH) in varying amounts. This reaction will be repeated over time producing an excess of CH. The fly ash will then consume the excess CH and continue to hydrate, forming additional C-S-H, and gaining additional strength over time. In a HVFA concrete, additional

calcium hydroxide is required to ensure a more complete hydration process for the fly ash.

The hydrated lime (calcium hydroxide) used in this study was purchased from the Mississippi Lime company located in Sainte Genevieve, MO. A standard hydrated lime material of 96% purity was added to the HVFA mixture. **Figure 3.2** shows the packaging and calcium hydroxide material.

Figure 3.2 – Calcium hydroxide material sample

The same method used for the selection of the amount of gypsum was repeated to determine the proportions for calcium hydroxide. Bentz found that at least 5 percent of calcium hydroxide by weight of cementitious material was sufficient for early and later strength gain in cement pastes containing a 50:50 ratio of portland cement to fly ash. Having higher fly ash content would likely require more than 5 percent calcium hydroxide, so it was decided to use a 10 percent replacement of fly ash with calcium

hydroxide. A higher amount of calcium hydroxide (15 percent) was also tested and initial results showed an increase in the compressive strength compared to the paste containing only 10 percent calcium hydroxide. However, results of compressive strength at later ages showed no advantageous increase, concluding that a 10 percent replacement with calcium hydroxide was sufficient for this particular fly ash.

3.4. PASTE AND MORTAR CUBES

3.4.1. General. The purpose of testing paste and mortar cubes was to optimize the constituent percentages for a control and experimental HVFA mix using a specimen that is smaller and more cost-effective to construct before advancing to larger specimen tests. Cubes made from paste (water, cementitious materials, and activators only) were used to determine what percentages of fly ash substitution, gypsum, and calcium hydroxide were optimal to achieve practical early-age compressive strengths. Mortar cubes, including sand supplied by Capital Sand in Jefferson City, were used to determine a plausible water to cement ratio that would allow for a sufficient balance between workability and compressive strength.

3.4.2. Paste Cubes Procedure. Each specimen was constructed and tested following the guidelines set forth in ASTM C109-08 using 2 in. (50 mm) cube specimens. The specimens were moist cured until the day of testing. The paste cubes, with a 0.40 *w/cm*, were tested at 1, 3, and 7 days in order to determine the early strengths of the mix, since early form removal is a concern when using HVFA concrete for construction. The 0.40 w/cm was selected based on previous research and the desired objectives of this stage of the research as mentioned previously. Several modifications

were made to the ASTM C109-08 procedure in order to account for the low paste viscosity and the addition of activators in the mixing phase. These modifications were as follows:

- To ensure that no paste would leak through the joints in the cube molds, the molds were caulked with silicon on the outside (**Figure 3.3**)
- A 5 gallon (19 L) bucket with lid was modified to accommodate a drill-driven paddle by cutting a hole in the lid (**Figure 3.4**)
- One half of the required mixing water was added to the bucket
- Cementitious materials were then added to the bucket (first the fly ash, then the cement) while stirring the mixture
- The activators (CH and gypsum) were mixed with the remaining half of the required water in a separate container to form a light slurry
- The activator slurry was then added to the cementitious mixture and mixed with the drill paddle for 5 minutes
- After mixing, the sides and lid of the bucket were checked for excess and unmixed material
- The mix was then transferred to a pitcher with a pouring spout for ease of placement into the cube molds
- The paste was then poured into the molds in one lift via the pitcher
- The molds were then vibrated with a rubber mallet for consolidation purposes and the excess paste was struck off with a polypropylene straight edge
- The molds were then placed in a moist cure chamber

- The cubes were de-molded at 1 day with the exception of the 100 percent fly ash specimens which had not set
- The de-molded cubes were placed back in the moist cure room until the test dates

Every specimen was tested on a 600,000 lb. (2,670 kN) capacity Forney compression machine until failure. The test matrix for this phase of the study is shown below in **Table 3.3**.

Figure 3.3 – Caulked cube molds

Figure 3.4 – 5 gallon bucket and mixer set-up

Table 3.3 – Test matrix for paste cubes

	% of Cementitious Material			
Specimen Set *	**Cement**	**Fly Ash**	**Gypsum**	**Calcium Hydroxide**
Control	100	0	-	-
50/50	50	50	-	-
40/60	40	60	-	-
25/75	25	75	-	-
100% FA	0	100	-	-
50/50-G	50	50	4	-
40/60-G	40	60	4	-
25/75-G	25	75	4	-
100% FA-G	0	100	4	-
50/50-G-10CH	50	50	4	10
40/60-G-10CH	40	60	4	10
25/75-G-10CH	25	75	4	10
100% FA-G-10CH	0	100	4	10
50/50-G-15CH	50	50	4	15
40/60-G-15CH	40	60	4	15
25/75-G-15CH	25	75	4	15
100% FA-G-15CH	0	100	4	15

3.4.3. Mortar Cubes Procedure. The mortar cubes, with *w/cm* values of 0.30 and 0.40, were tested at 3, 7, and 28 days (moist cured until test date) to predict the effects that the *w/cm* would have on the mix from the early strengths up until the design strength of 28 days. The mortar cube fabrication process more closely followed the ASTM C109-08 standard. Due to a more manageable mix viscosity, actual mixing was performed using a Hobart mixer. The activators were added, as they were for the paste cubes, as part of the second water addition, and the sand-to-cementitious material ratio used was 0.33. The sand gradation is shown in **Table 3.4**

Table 3.4 – Sand gradation performed at Missouri S&T

Sieve Size	⅜"	#4	#8	#16	#30	#50	#100	#200
Total % Passing	100	99	92	79	48	9	1	0.2

Every specimen was tested on a 600,000 lb. (2,670 kN) capacity Forney compression machine until failure. The test matrix for this experiment is shown below in **Table 3.5**.

Table 3.5 – Test matrix for mortar cubes

		% of Cementitious Material	
Specimen Set *	**w/cm**	**Cement**	**Fly Ash**
Control-0.40	0.4	100	0
50/50-0.40		50	50
25/75-0.40		25	75
100% FA-0.40		0	100
Control-0.30	0.3	100	0
50/50-0.30		50	50
25/75-0.30		25	75
100% FA-0.30		0	100

3.4.4. Results. The results recorded from the mortar and paste cube tests were organized into **Table**s **3.6** and **3.7**. Each value in the tables represents the average of three replicate specimens.

Table 3.6 – Compressive strengths for mortar cubes

		Compressive Strength (psi)		
Specimen Set	**w/cm**	**Day 3**	**Day 7**	**Day 28**
Control-0.40	0.40	3440	5280	5510
50/50-0.40		2730	4080	5370
25/75-0.40		1000	1910	2910
100% FA-0.40		74.0	313	520
Control-0.30	0.30	2905	4700	5110
50/50-0.30		2110	2180	3930
25/75-0.30		1430	1820	2380
100% FA-0.30		218	468	881

(1 psi = 6.89 kPa)

Table 3.7 – Compressive strengths for paste cubes

	Compressive Strength (psi)		
Specimen Set	**Day 1**	**Day 3**	**Day 7**
Control	1750	3920	5260
50/50	558	1920	3590
40/60	439	1570	2140
25/75	0	740	1270
100% FA	0	35	53
50/50-G	981	2500	3540
40/60-G	793	1700	2470
25/75-G	339	1270	1650
100% FA-G	0	0	71
50/50-G-10CH	1060	2530	2940
40/60-G-10CH	953	2240	2710
25/75-G-10CH	554	1220	1310
100% FA-G-10CH	671	670	748
50/50-G-15CH	1710	2650	3800
40/60-G-15CH	890	2390	3700
25/75-G-15CH	980	1080	1550
100% FA-G-15CH	624	616	580

(1 psi = 6.89 kPa)

3.4.5. Analysis and Conclusions. The test results from the mortar cubes suggest that using a *w/cm* of 0.30 can increase the specimen strength in some cases, such as with the 25/75 mix, but the loss of workability outweighs the minimal strength gain. This is evident with the 0.30 *w/cm* control specimens, which yielded lower results due to compaction problems caused by the lack of water. Therefore, a *w/cm* of at least 0.40 was selected for further testing. A graphical representation of this tests data is shown in **Figure**s **3.5** and **3.6**.

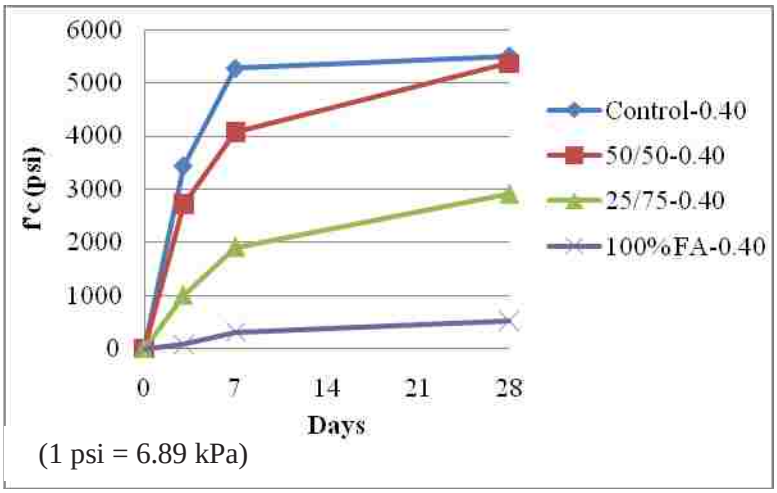

Figure 3.5 – Mortar cube compressive strengths on test days (*w/cm* = 0.40)

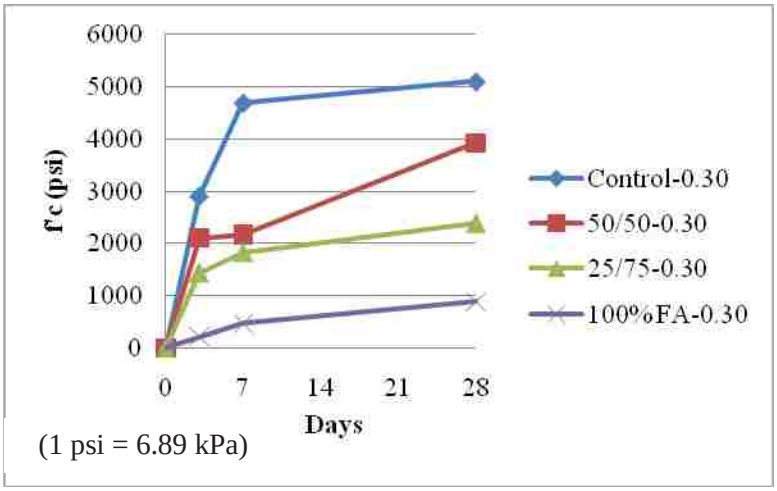

Figure 3.6 - Mortar cube compressive strengths on test days (*w/cm* = 0.30)

A number of conclusions can be drawn from the paste cube test data (**Figures 3.7** to **3.10**). The data shows that adding 15 percent calcium hydroxide and 4 percent gypsum (by weight of cementitious material) results in the highest compressive strengths for the HVFA mixes. The two best performing HVFA mixes were the 50 percent and 60 percent fly ash mixes with nearly identical 7 day strengths. The 75 percent fly ash mix did not perform as well as the 50 percent and 60 percent mixes, but exhibited sufficient strength at 7 days. The poorest performing mix was the 100 percent fly ash mix. Since the objective of this study was to push the bounds of fly ash substitution in concrete, the 75 percent fly ash mix was selected for further testing. The 75 percent fly ash mix including 10 percent calcium hydroxide was used since there was little difference in the results between this mix and the mix including 15 percent calcium hydroxide.

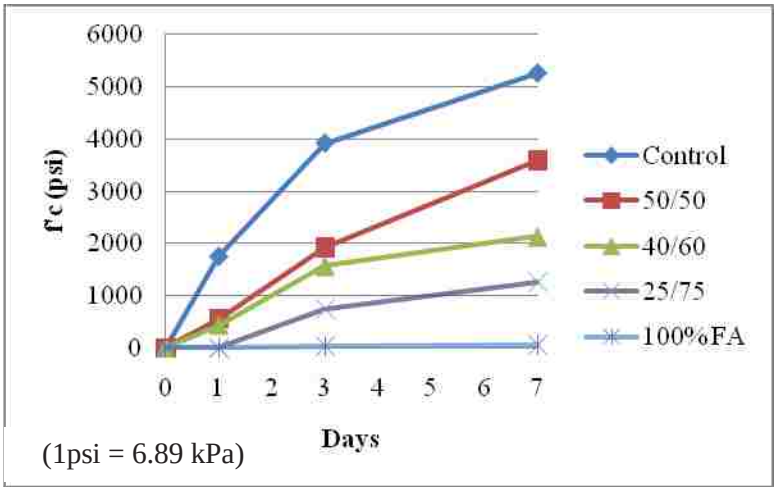

Figure 3.7 – Paste cubes with no admixtures

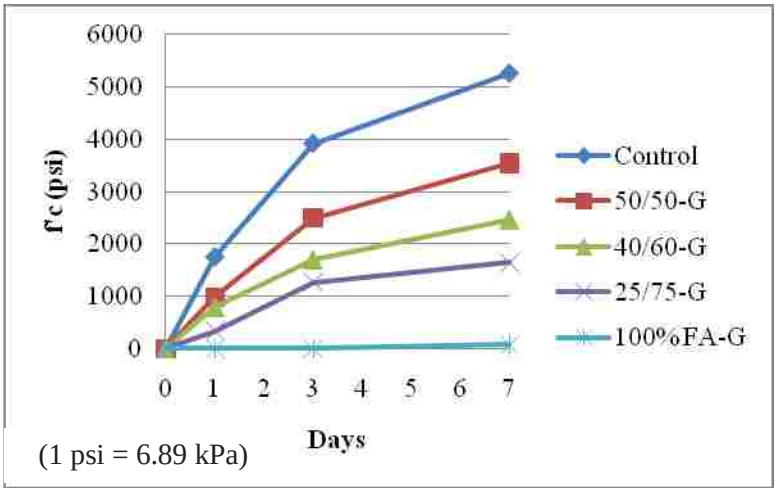

Figure 3.8 – Paste cubes with 4 percent gypsum

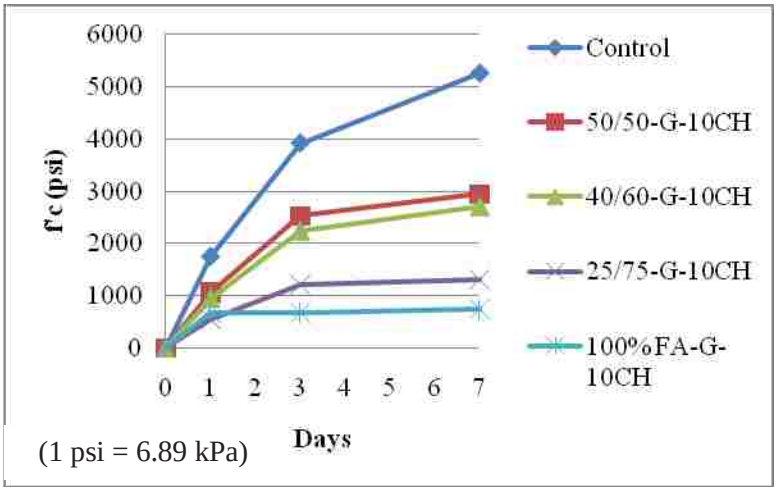

Figure 3.9 – Paste cubes with 4 percent gypsum and 10 percent calcium hydroxide

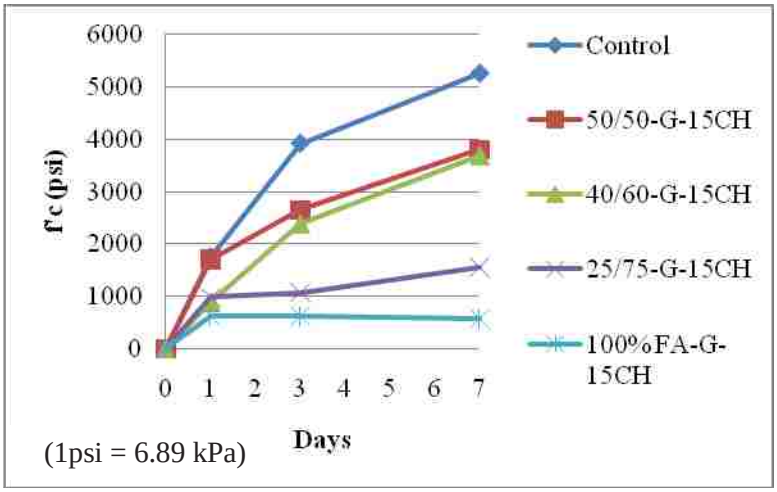

Figure 3.10 – Paste cubes with 4 percent gypsum and 15 percent calcium hydroxide

3.5. CONCRETE MIX DESIGN

The HVFA concrete mix design was developed using the procedure outlined in Section 6 of the ACI 211.1-91 document. The procedure for selection of mix proportions given in this document is applicable to normal weight concrete. Estimating the required

batch weights for the concrete involves a sequence of logical, straightforward steps to fit the characteristics of the materials into a mixture suitable for a specific application. An expected 28-day target strength of 5,000 psi (34.5 MPa) was considered. The solution approach used during the mix development is summarized below.

3.5.1. Choice of Slump. If slump is not specified, a value appropriate for the work can be selected from **Table 3.8**. These slump ranges shown apply when vibration is used to consolidate the concrete.

Table 3.8 – Recommended slump for various types of construction (ACI 211.1-91)

Types of construction	Slump (in.)	
	Maximum	Minimum
Reinforced foundation, walls, and footings	3	1
Plain footings, caissons, and substructure walls	3	1
Beams and reinforced walls	4	1
Building columns	4	1
Pavements and slabs	3	1
Mass concrete	2	1

(1 in = 25.4 mm)

The slump may be increased when chemical admixtures are used, provided that the admixture-treated concrete has the same or lower water-to-cement or water-to-cementitious materials ratio and does not exhibit segregation potential or excessive bleeding. For this research, a slump of 4 in. (102 mm) was selected.

3.5.2. Choice of Maximum Aggregate Size. The maximum aggregate size was determined based on the gradation of the materials available locally. A gradation of the coarse aggregate is shown in **Table 3.9**. Generally, the nominal maximum aggregate size

should be the largest that is economically available and consistent with the dimensions of the structure. Large nominal maximum sizes of well graded aggregates have fewer voids than smaller sizes. For this research, a coarse aggregate having a nominal maximum size of ¾ in. (19 mm) was considered.

Table 3.9 – Coarse aggregate gradation performed at Missouri S&T

Sieve Size	1”	¾”	½”	⅜”	#4	#8	#30	#100	#200
Total % Passing	100	89	59	47	16	7	4	4	3

3.5.3. Estimation of the Mixing Water and Air Content. The quantity of water per unit volume of concrete required to produce a given slump is dependent on: the nominal maximum size, particle shape, and gradation of the aggregates; the concrete temperature; the amount of entrained air; and the use of chemical admixtures. Slump is not significantly affected by the quantity of cement or cementitious materials within normal levels. The selection of the required mixing water was made based on **Table 3.10**.

Slump values of more than 7 in. (178 mm) are only obtained through the use of water-reducing chemical admixtures. For this research, a value of 340 lb/yd^3 (1978 N/m^3) of water was obtained from this table. This value was defined as the optimum value for this mix design. However, for concrete ordered from the local ready mix supplier, approximately 8 gallons per yd^3 (40 L/m^3) of water was held in abeyance for subsequent slump adjustment at the lab prior to placement. Water was then added at the lab until the desired slump was reached, but never exceeding the amount of water held back initially.

This approach also helped to adjust the overall mixing water content based on the actual water content of the aggregate for each particular placement.

Table 3.10 – Approximate mixing water and air content requirements for different slumps and nominal maximum sizes of aggregates (ACI 211.1-91)

Water (lb/yd^3) of concrete for indicated nominal maximum sizes of aggregate								
Slump (in.)	**⅜ in.**	**½ in.**	**¾ in.**	**1 in.**	**1½ in**	**2 in.**	**3 in.**	**6 in.**
Non-air-entrained concrete								
1 to 2	350	335	315	300	275	260	220	190
3 to 4	385	365	340	325	300	285	245	210
6 to 7	410	385	360	340	315	300	270	-
More than 7	-	-	-	-	-	-	-	-
Approximate amount of entrapped air in non-air-entrained concrete (%)	3.0	2.5	2.0	1.5	1.0	0.5	0.3	0.2
Air-entrained concrete								
1 to 2	305	295	280	270	250	240	205	180
3 to 4	340	325	305	295	275	265	225	200
6 to 7	365	345	325	310	290	280	260	-
More than 7	-	-	-	-	-	-	-	-
Recommended averages total air content, percent for level of exposure								
Mild exposure	4.5	4.0	3.5	3.0	2.5	2.0	1.5	1.0
Moderate exposure	6.0	5.5	5.0	4.5	4.5	4.0	3.5	3.0
Severe exposure	7.5	7.0	6.0	6.0	5.5	5.0	4.5	4.0

(1 in = 25.4 mm)

Slump values of more than 7 in. (178 mm) are only obtained through the use of water-reducing chemical admixtures. For this research, a value of 340 lb/yd^3 (1978 N/m^3) of water was obtained from this table. This value was defined as the optimum value for this mix design. However, for concrete ordered from the local ready mix supplier, approximately 8 gallons per yd^3 (40 L/m^3) of water was held in abeyance for subsequent slump adjustment at the lab prior to placement. Water was then added at the lab until the

desired slump was reached, but never exceeding the amount of water held back initially. This approach also helped to adjust the overall mixing water content based on the actual water content of the aggregate for each particular placement.

3.5.4. Selection of the Water-to-cementitious Materials Ratio. The *w/cm* is determined not only by strength requirements, but also by factors such as durability. In the absence of data to develop a relationship between strength and this ratio for the materials to be used, a set of approximate and relatively conservative values for concrete containing Type I portland cement can be taken from **Table 3.11**.

Table 3.11 – Relationship between water-to-cement or water-to-cementitious materials ratio and compressive strength of the concrete (ACI 211.1-91)

Compressive strength at 28 days (psi)	Water-to-cement ratio by weight	
	Non-air-entrained concrete	Air-entrained concrete
6,000	0.41	-
5,000	0.48	0.40
4,000	0.57	0.48
3,000	0.68	0.59
2,000	0.82	0.74

(1 psi = 68.9 kPa)

These values are estimated average strengths for concrete containing no more than 2 percent air for non-air-entrained concrete and 6 percent total air content for air-entrained concrete. Strength is based on 6 × 12 in. (152 mm x 305 mm) cylinders moist-cured for 28 days. The relationship in **Table 3.11** assumes a nominal maximum aggregate size of about ¾ (19 mm) to 1 inch (25 mm). For this research, two water-to-cement ratios were used. A water-to-cement ratio (*w/c*) of 0.45 was selected for the conventional mix,

and a water-to-cementitious materials ratio (*w/cm*) of 0.40 was selected for the HVFA mix. This difference in these ratios is due to reports of previous research showing that when fly ash is incorporated into the mix, the water demand is lower for the same level of workability.

3.5.5. Calculation of the Cement Content. The amount of cement per unit volume of concrete is fixed by the determinations made in Section 3.5.3 and 3.5.4 above. The required cement is equal to the estimated mixing-water content divided by the water-to-cement ratio. Equation 3-1 shows how to calculate the amount of cement.

$$Amount\ of\ cement = \frac{340}{0.40} = 850\ {}^{lb}/_{yd^3} \quad (3\text{-}1)$$

3.5.6. Estimation of the Coarse Aggregate Content. Aggregates of essentially the same nominal maximum size and gradation will produce concrete of satisfactory workability when a given volume of coarse aggregate is used per unit volume of concrete. Appropriate values for this aggregate volume are given in **Table 3.12**. The volume of coarse aggregate in a unit volume of concrete is dependent only on its nominal maximum size and the fineness modulus of the fine aggregate. The fineness modulus of the fine aggregate available from the local supplier was 2.60.

Volumes are based on aggregates in oven-dry-rodded conditions. These volumes are selected from empirical relationships to produce concrete with a degree of workability suitable for usual construction.

For this research, the available coarse aggregate had a unit weight of 101.5 lb/ft^3 (591 N/m^3). The amount of coarse aggregate is calculated from the value obtained in

Table 3.12 multiplied by 27 and the unit weight. Equation 3-2 shows how to calculate the amount of coarse aggregate.

Table 3.12 – Volume of coarse aggregate per unit of volume of concrete (ACI 211.1-91)

Nominal maximum size of aggregate (in.)	Volume of oven-dry-rodded coarse aggregate per unit volume of concrete for different fineness moduli of fine aggregate			
	2.40	*2.60*	*2.80*	*3.00*
⅜	0.50	0.48	0.46	0.44
½	0.59	0.57	0.55	0.53
¾	0.66	0.64	0.62	0.60
1	0.71	0.69	0.67	0.65
1½	0.75	0.73	0.71	0.69
2	0.78	0.76	0.74	0.72
3	0.82	0.80	0.78	0.76
6	0.87	0.85	0.83	0.81

(1 in = 25.4 mm)

$$Amount\ of\ coarse\ aggregate = 0.64 \times 27 \times 101.5 = 1750\ {}^{lb}/_{yd^3} \quad (3\text{-}2)$$

3.5.7. Estimation of the Fine Aggregate Content. After the completion of the previous step, all ingredients of the concrete have been estimated except for the fine aggregate. Either of two procedures may be employed to estimate the fine aggregate content, the weight method or the absolute volume method. For this research, the weight method was used.

The required weight of the fine aggregate is simply the difference between the weight of fresh concrete calculated using **Table 3.13** and the total weight of the other ingredients. Equation 3-3 shows how to calculate the amount of fine aggregate.

Table 3.13 – First estimate of weight of fresh concrete (ACI 211.1-91)

Nominal maximum size of aggregate (in.)	First estimate of weight of fresh concrete (lb/yd^3)	
	Non-air-entrained concrete	Air-entrained concrete
⅜	3840	3710
½	3890	3760
¾	3960	3840
1	4010	3850
1½	4070	3910
2	4120	3950
3	4200	4040
6	4260	4110

(1 in = 25.4 mm, lb/ft^3 = 157 N/m^3)

$$Amount\ of\ fine\ aggregate = 3960 - (340 + 850 + 1754) = 1020\ {}^{lb}/_{yd^3} \qquad (3\text{-}3)$$

3.5.8. Adjustments for Aggregate Moisture. The aggregate quantities to be weighed out for the concrete must allow for moisture in the aggregates. Generally, the aggregates will be moist and their dry weights should be increased by the percentage of water they contain, both absorbed and surface. The mixing water added to the batch must be reduced by an amount equal to the free moisture contributed by the aggregate.

During the casting of the beams, periodic measurements of moisture content and percentage of absorption were carried out on the coarse and fine aggregates to maintain

the same conditions for all castings. The moisture content was measured following the standard described in ASTM C566, Standard Test Method for Total Evaporable Moisture Content of Aggregate by Drying (ASTM C 566, 1997). The percentage of absorption was measured following the standards described in ASTM C127, Standard Test Method for Density, Relative Density (Specific Gravity), and Absorption of Coarse Aggregate (ASTM C127, 2007) for the coarse aggregate and ASTM C128, Standard Test Method for Density, Relative Density (Specific Gravity), and Absorption of Fine Aggregate (ASTM C128, 2007) for the fine aggregate. Equations 3-4 through 3-6 show how to adjust the amount of water due to moisture contents. As an example, data measured in the first and second castings of the control specimens will be used, the moisture contents for the coarse aggregate and fine aggregate measured 2.3 percent and 1.7 percent, respectively. The percentages of absorption were found to be 0.5% and 0.9% for the coarse and fine aggregate, respectively. Absorbed water does not become part of the mixing water, therefore, it is excluded from the adjustment in the water as shown below.

$$Adjustment\ for\ coarse\ aggregate = 1754 \times (0.023 - 0.005) = 31.6\ ^{lb}/_{yd^3} \quad (3\text{-}4)$$

$$Adjustment\ for\ fine\ aggregate = 1016 \times (0.017 - 0.009) = 8.1\ ^{lb}/_{yd^3} \quad (3\text{-}5)$$

$$Amount\ of\ water\ (adjusted) = 340 - (31.6 + 8.1) = 300.3\ ^{lb}/_{yd^3} \quad (3\text{-}6)$$

3.5.9. Estimation of the Amount of Fly Ash, Calcium Hydroxide, and Gypsum.

This step does not apply to the control specimens that were cast using a conventional mix. The purpose of this research was to evaluate the effectiveness of a concrete containing a high amount of fly ash. After some batching and testing of different

mixes using cubes and cylinders, a 70 percent replacement of portland cement with fly ash was selected as the target. Additional powder activators to improve the early strength were also considered in the mix design. Calcium hydroxide and gypsum were selected for their favorable contribution to the development of early strength in a high-volume fly ash concrete mix. A 10 percent replacement with calcium hydroxide and a 4 percent replacement with gypsum were incorporated to the mix design. The amount of these activators was based on the amount of fly ash, but it was deducted from the total amount of the cementitious materials to maintain the ratio between the fly ash and portland cement (70/30). Equations 3-7 through 3-11 show how to calculate the weight of these admixtures. From equation 3-1, a total amount of cement equal to 850 lb/ft^3 (13660 kg/ ft^3) was determined for the base (control) mix design.

$$Amount\ of\ fly\ ash\ (not\ final) = 850 \times 0.70 = 595\ {}^{lb}/_{yd^3} \quad (3\text{-}7)$$

$$Amount\ of\ calcium\ hydroxide = 595 \times 0.10 = 59.5\ {}^{lb}/_{yd^3} \quad (3\text{-}8)$$

$$Amount\ of\ gypsum = 595 \times 0.04 = 23.8\ {}^{lb}/_{yd^3} \quad (3\text{-}9)$$

$$Amount\ of\ fly\ ash\ (final) = \left(850 - (59.50 + 23.80)\right) \times 0.70 = 537\ {}^{lb}/_{yd^3} \quad (3\text{-}10)$$

$$Amount\ of\ cement = \left(850 - (59.50 + 23.80)\right) \times 0.30 = 230\ {}^{lb}/_{yd^3} \quad (3\text{-}11)$$

3.5.10. Summary of the Mix Designs. Tables **3.14** and **3.15** present a summary of the final amount of each ingredient for the mixes used in this research. **Table 3.14** presents the final design of a conventional mix used in the control specimens with a *w/c*

equal to 0.45. **Table 3.15** presents the final design of the HVFA concrete mix used in this research with a *w/cm* equal to 0.40. The values contained in these tables are given in saturated surface dry (SSD) conditions.

Table 3.14– Conventional mix description

Ingredient	Amount (lb/ft^3)
Water	340
Portland cement	756
Coarse aggregate	1750
Fine aggregate	1110
w/c	0.45

(lb/ft^3 = 16 kg/m^3)

Table 3.15 – HVFA mix description

Ingredient		Amount (lb/ft^3)
Water		340
Cementitious materials	Portland cement	230
	Fly ash	537
	Calcium hydroxide	59.5
	Gypsum	23.8
Coarse aggregate		1750
Fine aggregate		1110
w/cm		0.40

(lb/ft^3 = 16 kg/m^3)

3.6. CYLINDER COMPRESSION TESTING

3.6.1. General. Cylinder compression tests were used to test the strengths of the mixes utilizing the proportions from the compression cube tests in conjunction with the other concrete constituents, such as coarse and fine aggregate. A mix with a fly ash

replacement value of 70 percent was selected for testing based on the success of the 75 percent fly ash paste cube specimens. This design allows the mix to have a fly ash percentage closer to that of the top performing HVFA paste cube specimens as well as a fly ash content twice the ACI recommended maximum of 35 percent (ACI Committee 232, 2003). Four other sets of cylinders were constructed using fly ash replacement contents of 0, 50, 60, and 75 percent for comparison purposes.

3.6.2. Procedure. Each cylinder specimen was constructed in accordance with ASTM C192, Standard Practice for Making and Curing Concrete Test Specimens in the Laboratory (ASTM C192, 2007). Mixing was performed in a 4 cubic foot (0.11 cubic meter) drum mixer (**Figure 3.11**). The fly ash was added with the cement at the ASTM designated time for addition of cementious material and the activators were added using the second specified water addition as a vehicle. The concrete was then mixed, poured, and cured as per ASTM C192 (2007). The specimens were moist cured for 1, 3, 7, or 28 days, depending on the designated test day for each specimen, before they were tested until failure using a 600,000 lb. (2,670 kN) capacity Forney compression machine in accordance with ASTM C39-09. The test matrix for the cylinder tests is shown in **Table 3.16**.

3.6.3. Results. The results from the cylinder compressive strength tests are shown in **Table 3.17**. As with the compression cube tests, each specimen set consists of the average of three replicate specimens.

3.6.4. Analysis and Conclusions. The test results, as shown in **Figure 3.12**, suggest that the highest strength HVFA concrete mixes are the 50 and 60 percent fly ash proportions with nearly identical results. The 70 percent fly ash mix, however, yielded a

reasonable 1-day compressive strength of over 1100 psi (7.58 MPa), a 3-day compressive strength of nearly 2000 psi (13.8 MPa), and 28-day strength of nearly 4500 psi (31 MPa). Since these values are acceptable when designing concrete for normal construction, the final HVFA concrete mix chosen for this study was the 70 percent fly ash mix with 4 percent gypsum and 10 percent calcium hydroxide.

Figure 3.11 – Large drum mixer

Table 3.16 – Test matrix for cylinder compression tests

		Cementitious Materials (%)			
Specimen Set *	w/cm	Fly Ash	Cement	Gypsum	CH
Control	0.45	0	100	4	10
HVFA (50%)	0.40	50	50	4	10
HVFA (60%)	0.40	60	40	4	10
HVFA (70%)	0.40	70	30	4	10
HVFA (75%)	0.40	75	25	4	10

Table 3.17 – Test results from cylinder compression tests

		Compressive Strength (psi)			
Specimen Set *	**w/c**	**Day 1**	**Day 3**	**Day 7**	**Day 28**
Control	0.45	3090	4540	5180	6190
HVFA (50%)	0.40	1190	2460	3980	5360
HVFA (60%)	0.40	1240	2670	3990	5480
HVFA (70%)	0.40	1120	1850	2880	4430
HVFA (75%)	0.40	660	1230	2000	3020

*Each set is comprised of the average of three specimens
(1 psi = 6.89 kPa)

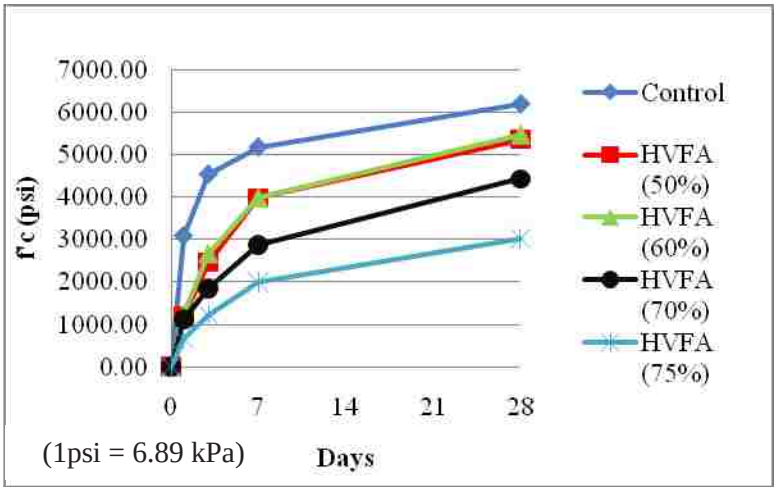

Figure 3.12 – Compressive strength vs. test day plot for all cylinder mixes

3.7. FINAL MIX DESIGN AND MIXING DETAILS

Concrete for this study was provided by a ready mix plant, Rolla Ready Mix, in order to emulate field construction practices. The mix design provided to Rolla Ready Mix was decided upon based on the results described in Sections 3.4 and 3.6, only

batched at a higher quantity, but using the same constituent proportions. The control mix was a 100 percent portland cement mix that was completely batched at the ready mix plant. The high-volume fly ash concrete mix featured a 70 percent replacement of cement with fly ash. The quantities used for each pour are shown in **Table**s **3.13** and **3.14** with only a difference in the amount of water that was adjusted based on the moisture content and percentage of absorption measured in both fine and coarse aggregates. While the fly ash was added at the ready mix plant, the required amounts of gypsum and calcium hydroxide, as per Section 3.4, were added directly to the truck upon arrival to the lab. Once mixed thoroughly for a minimum of 5 minutes at high speed, the concrete placement commenced. During each placement, a slump tests was performed to ensure the workability of the concrete. A 6-inch (152 mm) slump was the typical target value. Also, as a part of the concrete placement, cylinders were cast in order to test the compressive strength at 28 days and on the day of testing of the full-scale specimens. **Figure 3.13** presents a summary of images showing the construction process followed during each casting.

(a) Adding gypsum

(b) Adding calcium hydroxide

(c) Concrete placement

Figure 3.13 – HVFA concrete procedures

4. PULL-OUT TEST

4.1. INTRODUCTION

The goal of the experimental program was to perform comparative bond tests on high-volume fly ash concrete and conventional (control) concrete. The first test performed was the pull-out test. Although there are a variety of bond and development length testing protocols available, a direct pull-out test offers several advantages, including test specimens that are easy to construct and a testing method that is relatively simple to perform. The downside is a lack of direct comparison with actual structures and the development of compressive and confinement stresses generated due to the reaction plate. However, modifications suggested in RILEM 7-II-128 (1994) reduce some of these problems and result in a simplified test that offers relative comparisons between concrete or reinforcement types. Bond between the reinforcing bar and the concrete only occurs in the upper half of the concrete block, significantly reducing the effect of any confinement pressure generated as a result of friction between the specimen and the reaction plate.

The following section describes in detail the form development, specimen construction, test process, results, and conclusions for the pull-out tests.

4.2. SPECIMEN DESIGN AND FABRICATION

4.2.1. Pull-out Specimen Parameters. The pull-out specimens were designed using RILEM7-II-128 (1994) as a guide. The bars were embedded 10 times the bar diameter into the concrete specimen based on preliminary testing, with half of the length

debonded using PVC. RILEM also recommends casting the bars into concrete cubes that provide a clear cover of 4.5 times the bar diameter from the bar to the center of each side of the horizontal cross section. The specimens designed for this experiment exceeded the RILEM requirement on clear cover and featured a 12-inch-diameter (305 mm) concrete cylinder to eliminate the potential for splitting and ensure that all of the specimens failed in the same manner (pull-out). Specimen dimensions for each bar size tested – No. 4 (No. 13) and No. 6 (No. 19) – are shown in **Figures 4.1** and **4.2.**

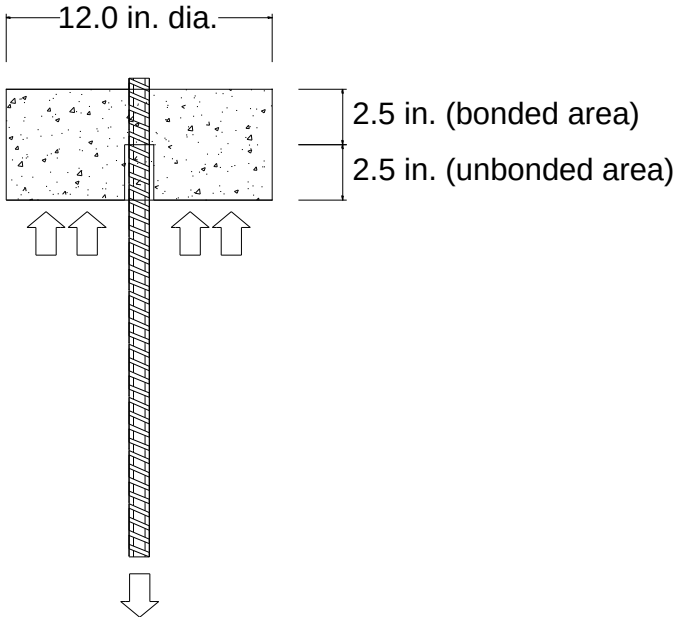

Figure 4.1 – Dimensions for pull-out specimen testing No. 4 bar

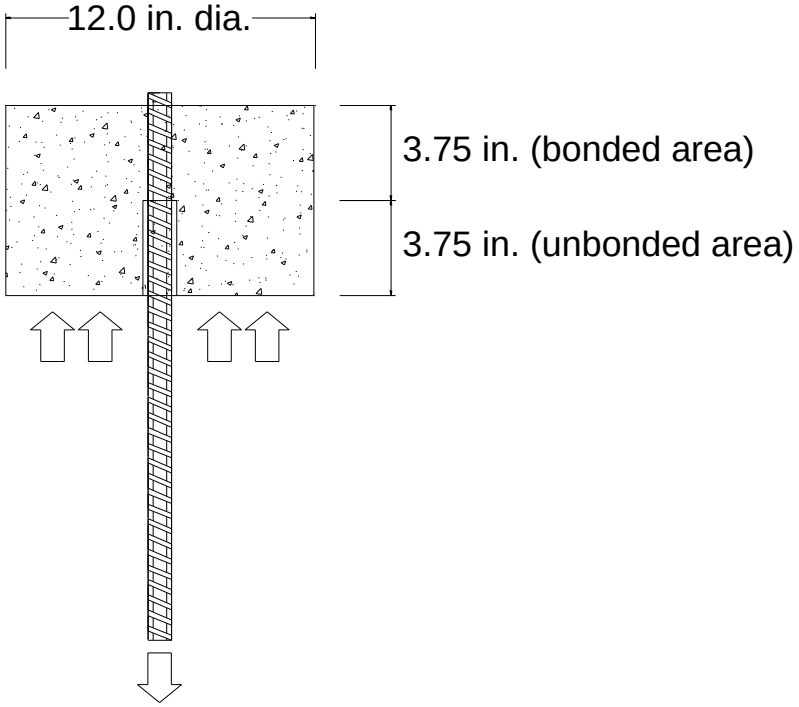

Figure 4.2 – Dimensions for pull-out specimen testing No. 6 bar

4.2.2. Pull-out Specimen Fabrication. Pull-out tests were performed on both the control and the high-volume fly ash concrete mixes using No. 4 and No. 6 bars. The variance in bars was included in order to observe the bond behavior of different size bars. The test matrix is shown in **Table 4.1**.

Each form was constructed using two 14 x 14-inch-squares (356 mm) of 1/2-inch-thick (13 mm) plywood, PVC pipe, ASTM A615-09 Grade 60 reinforcing bar, and prefabricated cardboard tubes (Quik-Tube). First, a hole, slightly larger than the bar cross-section, was drilled into each plywood square. Next, the Quik-Tube was cut to the height required for the specimen and glued to the first plywood square (centered). Each reinforcing bar was cut to a length of 40 in. (1016 mm) and fitted with a section of PVC

using tape and cardboard spacers. The PVC was half of the height of the specimen and taped to the rebar so that the top of the PVC was flush with the top of the form when the bar was placed in the hole in the base. Concrete was then placed into the form, rodded, and tamped. The second piece of plywood was then guided down the rebar and placed on the top of the Quik-Tube (**Figure 4.3**). Magnetic levels were used to ensure that the bar was perfectly centered and vertical. Finally, the specimens were covered with wet burlap and plastic, and then allowed to cure (**Figure 4.4**).

Table 4.1 – Pull-out test matrix

Specimen Name	Mix Type	Bar Diameter (in)
CPO_4-1	Control	0.5
CPO_4-2	Control	0.5
CPO_4-3	Control	0.5
FAPO_4-1	HVFA	0.5
FAPO_4-2	HVFA	0.5
FAPO_4-3	HVFA	0.5
CPO_6-1	Control	0.75
CPO_6-2	Control	0.75
CPO_6-3	Control	0.75
FAPO_6-1	HVFA	0.75
FAPO_6-2	HVFA	0.75
FAPO_6-3	HVFA	0.75

(1 in = 25.4 mm)

4.3 TEST SETUP AND PROCEDURE

4.3.1. Pull-out Test Setup. The pull-out specimens were loaded into a 200,000-pound-capacity (890 kN) Tinius Olson machine by rotating the specimen 180°, bar side

down, and threading the bar through a thin piece of rubber and the head of the machine until the specimen rested evenly on the rubber. The free end of the bar was clamped into a lower component of the Tinius Olson machine (**Figure 4.5**). A magnetic arm holding a DCDT was then placed on top of the specimen. The DCDT was placed directly on the 1/2 inch (13 mm) of exposed rebar on the back end of the specimen to record slip (**Figure 4.6**).

Figure 4.3 – Pull-out formwork

Figure 4.4 – Pull-out specimens

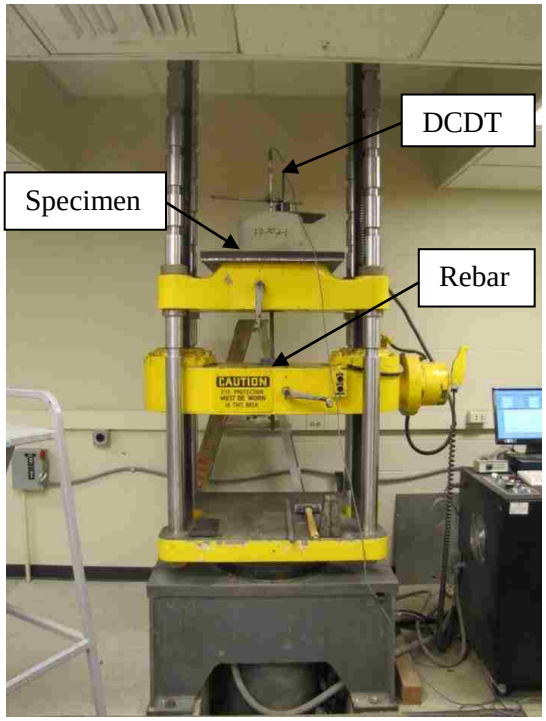

Figure 4.5 – Pull-out test setup with specimen loaded

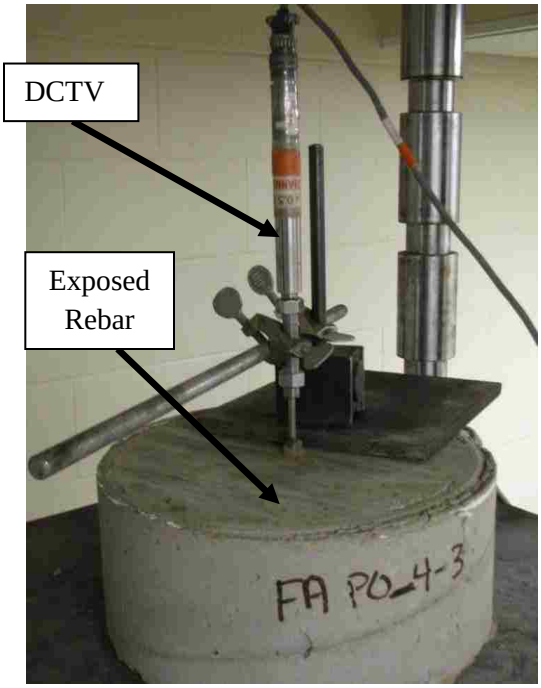

Figure 4.6 – DCDT setup

4.3.2. Pull-out Test Procedure. The Tinius Olson was set to pull on the rebar at a rate of 0.1 in. (2.5 mm) per minute to avoid any dynamic effect and in order to insure a sufficient number of data points before failure. The load was recorded on a data acquisition computer linked to the test machine. The DCDT was also monitored to record the slip as a function of load. The specimens were tested until a maximum load was reached. A photograph of a typical failed specimen is shown in **Figure 4.7**. All specimens failed without splitting of the concrete.

Figure 4.7 – Failed pull-out specimen

4.4. TEST RESULTS

The data recorded from the pull-out tests involved load and corresponding slip of the bar. This data was then organized in two different ways. First, the load vs. slip was plotted for each specimen, with a typical graph shown in **Figure 4.8**. All specimens

exhibited a similar plot for these variables in regard to the shape of the data points. The only major variance was the magnitude of the values. **Table 4.2** contains the maximum values for the pull-out load of each specimen as taken from the load vs. slip data and includes the average and coefficient of variation (COV) for each group of specimens. A t-test performed on this data at an alpha value of 0.05 and the results are available in Appendix D. According to the t-test, the data averages for the No. 6 bars (No. 19 bars) are statistically identical. The analysis for the No. 4 bar (No. 13 bar) specimens indicates that the averages are slightly different, but this could be due to the small sample size.

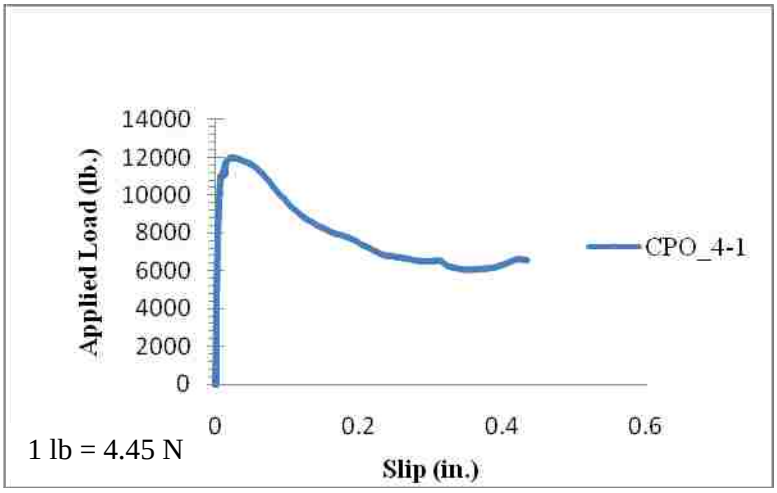

Figure 4.8 – Typical load vs. slip plot

Table 4.3 contains the compressive strength test data for each concrete pour and includes the average and COV for each group of specimens.

Table 4.2 – Pull-out test results

Specimen	Peak Load (lb)	Average Load (lb)	COV (%)
CPO_4-1	11994	11817	2.6
CPO_4-2	11989		
CPO_4-3	11469		
FAPO_4-1	10830	11079	2.0
FAPO_4-2	11183		
FAPO_4-3	11225		
CPO_6-1	32099	32624	1.4
CPO_6-2	32854		
CPO_6-3	32920		
FAPO_6-1	28471	27248	4.3
FAPO_6-2	27154		
FAPO_6-3	26119		

(1 lb = 4.45 N)

Table 4.3 – Compressive strength test data

	Test Day Strength (psi)				
	Cylinder 1	**Cylinder 2**	**Cylinder 3**	**Average**	**COV (%)**
All FAPO	4390	4140	4750	4420	7.0
All CPO	5660	5900	5720	5760	2.2

(1 psi = 6.89 kPa)

The maximum load for each individual test is plotted in **Figures 4.9** (control) and **4.10** (HVFA concrete). As shown in the plots, the test results were very similar from specimen to specimen with the same parameters. Therefore, the results for these tests

were extremely consistent. For instance, for the control specimens with the 1/2-inch-diameter (13 mm) bars, the range of data varied by only 525 pounds (2335 N) for an average bond strength of 11,820 pounds (52,562 N).

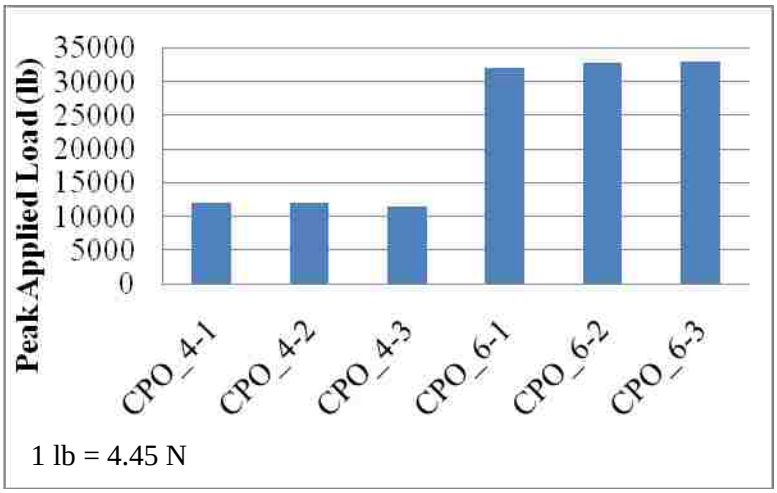

Figure 4.9 – Control peak load vs. specimen bar chart

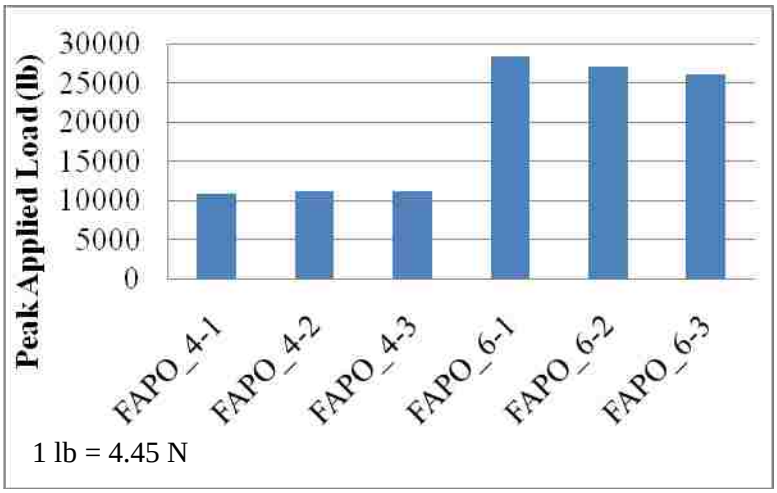

Figure 4.10 - HVFA peak load vs. specimen bar chart

4.5. DATA ANALYSIS AND INTERPRETATION

The results for the pull-out tests at first seemed to favor the control mix in terms of bond strength. However, since the compressive strength of the concrete mix is a significant contributing factor to bond strength, and each mix had a different compressive strength, a modification was made to the results. Each failure load was divided by the square root of the mix's test day compressive strength (√f'c) because of the relationship between bond strength and √f'c developed in Equation 12-1 of ACI 318 (2008). (**Equation 4.1**). A report by the Transportation Research Board (Ramirez and Russell, 2008) also describes extensive research performed on this method of equalization. According to the research, dividing the bond strength by √f'c is an acceptable method of modifying specimen results for a more direct comparison. Therefore, the loads recorded for the pull-out tests were divided by √f'c to negate the effect of differing compressive strengths. The results are shown in **Table 4.4**. Complete results for each test can be found in **Appendices A** and **B.**

$$l_d = \left(\frac{3}{40} \frac{f_y}{\lambda \sqrt{f'_c}} \frac{\psi_t \psi_e \psi_s}{\left(c_b + \frac{K_{tr}}{d_b} \right)} \right) d_b \qquad (4.1)$$

where:

l_d = development length

f_y = specified yield strength of reinforcement

λ = light weight concrete modification factor

f'_c = specified compressive strength of concrete

ψ_t = reinforcement location modification factor

ψ_e = reinforcement coating modification factor

ψ_s = reinforcement size modification factor

c_b = the smaller of: the distance from the centroid of a bar to the nearest concrete surface and the center to center spacing of bars being developed.

K_{tr} = transverse reinforcement index

d_b = bar diameter

Table 4.4 – Pull-out test results with modified loads

Specimen	Max Load (lb)	Concrete Compressive Strength (psi)	Modified Load (lb/√(psi)	Average Modified Load (lb/√(psi)	COV (%)
CPO_4-1	11994	5762	158	156	2.6
CPO_4-2	11989		158		
CPO_4-3	11469		151		
FAPO_4-1	10830	4424	163	167	2.0
FAPO_4-2	11183		168		
FAPO_4-3	11225		169		
CPO_6-1	32099	5762	423	430	1.4
CPO_6-2	32854		433		
CPO_6-3	32920		434		
FAPO_6-1	28471	4424	428	410	4.3
FAPO_6-2	27154		408		
FAPO_6-3	26119		393		

(1 lb = 4.45 N, 1 psi = 6.89 kPa, 1 lb/√(psi) = 8.36 N/√(Pa))

4.5.1. Load Analysis. Based solely on the modified peak load, the results for the pull-out tests were very similar and are shown in **Figure 4.11**. The HVFA concrete specimens failed at loads slightly higher for the 1/2-inch-diameter (13 mm) bar [167

lb/√psi (9.0 N/√Pa) vs. 156 lb/√psi (8.4 N/√Pa)], but the control specimen results were slightly higher for the 3/4-inch-diameter (19 mm) bar [430 lb/√psi (23 N/√Pa) vs. 410 lb/√psi (22 N/√Pa)]. The difference between the results is well within the accuracy of the test method and indicates nearly identical results between the two concrete types.

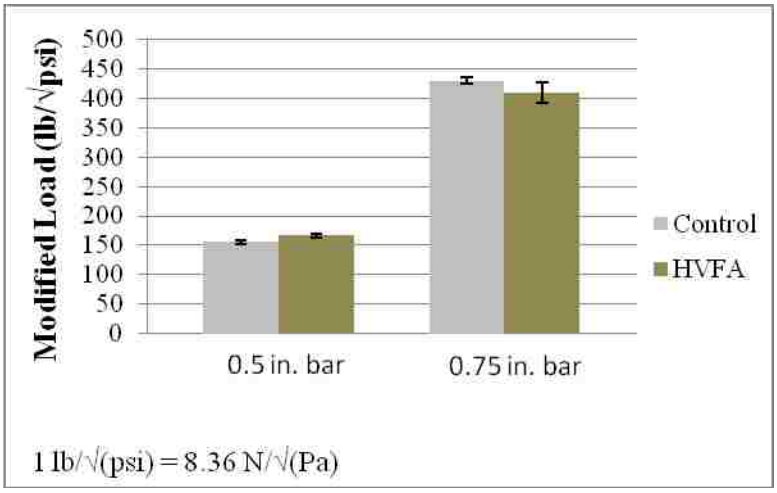

Figure 4.11 – Average specimen load comparison bar chart

4.5.2. Slip Analysis. Bar slip became evident at about the same modified load for each specimen, HVFA and control. Because the failure mode was pull-out for every specimen without any splitting, the similar slip behavior indicates that the concrete around the rebar ribs crushed at about the same load for each compared specimen. **Figure 4.12** shows a typical load vs. slip comparison between the two mixes using a 1/2-inch-diameter (13mm.) bar. One characteristic to note from this graph is that the control specimens appeared to maintain a higher load as the bar slipped out of the cylinders.

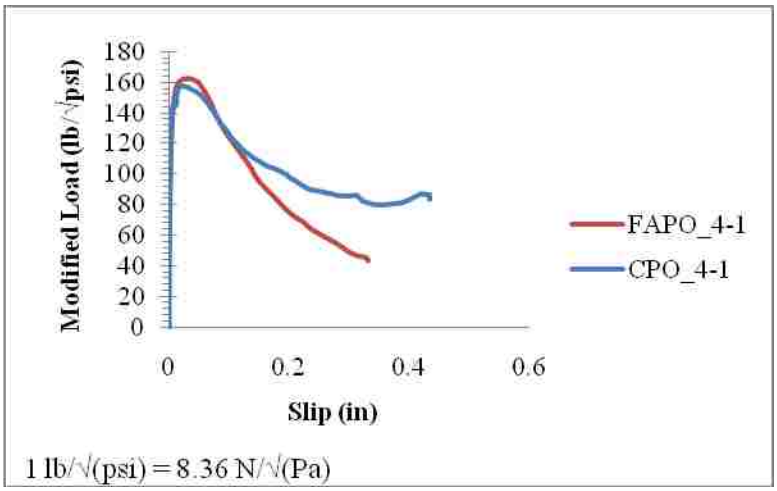

Figure 4.12 – Pull-out load vs. slip plot

4.6. CONCLUSIONS

The data recorded from the pull-out tests supports the effectiveness of HVFA concrete in terms of bond integrity. Since the pull-out test is a comparative test, this conclusion can be drawn based on the fact that the HVFA specimens demonstrated similar bond strengths to the control specimens (based on maximum modified load applied). The only drawback from testing was that once the concrete began to crush around the reinforcing bar, slip occurred at a higher rate for the HVFA specimens.

5. BEAM SPLICE TEST

5.1. INTRODUCTION

One downside to the pull-out test, as mentioned in Section 2, is that it alters the bond behavior due to factors that are not present in the field, making the pull-out test more useful for comparisons than for actual bond behavior. Therefore, the beam splice test was also performed to counter some of the inaccuracies of the pull-out test. As noted in Section 2, the beam splice test is generally regarded as the most realistic test method, and the current ACI 318 (2008) design provisions for development length and splice length are based primarily on data from this type of test setup (ACI Committee 408, 2003; Ramirez and Russell, 2008).

The following section describes in detail the form development, specimen construction, test process, results, and conclusions for the beam splice tests.

5.2. TENSILE TESTS

Tensile tests were performed to investigate material properties such as yield stress and strain for the No. 6 (No. 19) reinforcing bars used in the beam splice tests. The testing was performed using a 200,000 pound (890 kN) capacity Tinius-Olson universal compression/tension machine in accordance with ASTM E8-09, Standard Test Methods for Tension Testing of Metallic Materials (ASTM E8, 2009), and the results are shown in **Table 5.1.** The yield strains found from this test were later used to determine whether or

not the reinforcement in the beam splice tests yielded before bond failure, while the yield strengths were used to predict the failure loads for the beams.

Table 5.1 - Tensile test results

Specimen	Peak Load (kips)	Yield Strength (ksi)	Yield Strain (in/in)
1	41402	72	0.0026
2	42157	78	0.0024
3	41983	77	0.0026
4	47228	68	0.0020
5	46891	68	0.0020
6	47106	68	0.0020
Averages	44461	72	0.0023

(1 kip = 4.45 kN, 1 ksi = 6.89 MPa, 1 in = 25.4 mm)

5.3. SPECIMEN DESIGN AND FABRICATION

5.3.1. Splice Specimen Design. The beams for the splice test were modeled after provisions in ACI 408R (2003) using dimensions and bar spacings similar to splice tests performed in previous research (Russell and Ramirez, 2008). The beams measured 14 feet (4267 mm) long with a 12 x 18 inch (305 mm x 457 mm) rectangular cross-section. The cage was comprised of six No. 6 bars, lap spliced in the center and hooked at the ends to form three total longitudinal reinforcing bars. The splice length was determined using Equation 12-1 from the ACI 318 code (2008). The equation was solved using the specifications for this specimen, multiplied by 1.3 for a Class B splice, and then divided by two to obtain a splice length of 16.55 in. (420 mm). The reason that the ACI required splice length was divided by two was to ensure that the specimens failed due to bond and not yielding of the steel. The cages without confinement contained No. 3 bars for shear

reinforcement up until the splice on either side. Stirrups were installed across the splice on the confinement specimens. Shear reinforcement was designed to guarantee that the specimen failed due to the splice. Cage dimensions along with stirrup spacing and strain gage locations are detailed in **Figures 5.1** and **5.2.**

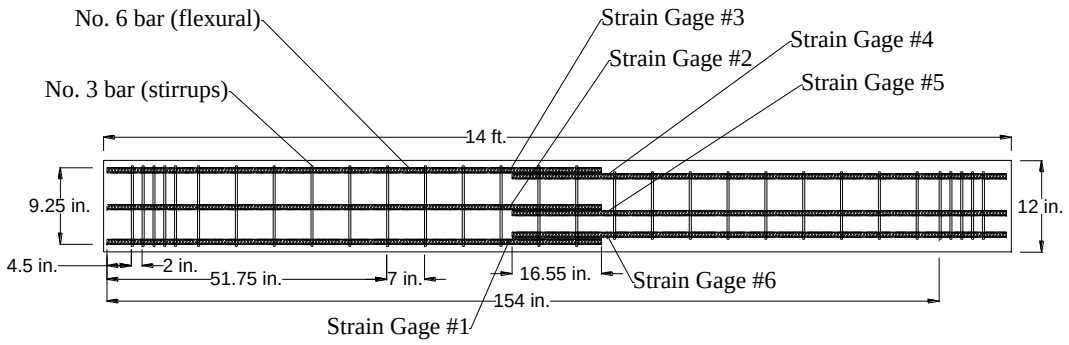

Figure 5.1 – Splice cage with no confinement (from above)

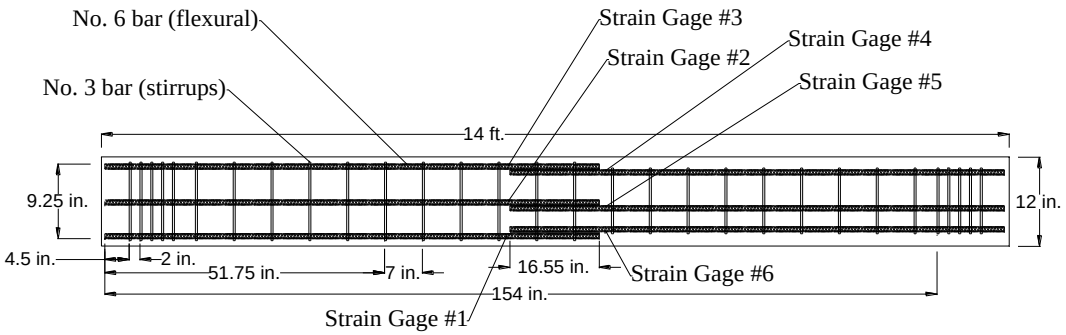

Figure 5.2 – Splice cage with confinement (from above)

5.3.2. Splice Specimen Fabrication. The splice tests were split into two groups. Half of the splice specimens included confinement along the splice length for both mixes, and the other half did not. The splices' reaction to confinement was tested due to ACI's inclusion of a confinement variable in the development equation (Equation 12-1 from ACI 318-08)**.** The test matrix is shown in **Table 5.2.**

Table 5.2 – Splice test matrix

Specimen Name	Mix Type	Confinement
CONT_NC-1	Control	No
CONT_NC-2	Control	No
CONT_NC-3	Control	No
FA_NC-1	HVFA	No
FA_NC-2	HVFA	No
FA_NC-3	HVFA	No
CONT_C-1	Control	Yes
CONT_C-2	Control	Yes
CONT_C-3	Control	Yes
FA_C-1	HVFA	Yes
FA_C-2	HVFA	Yes
FA_C-3	HVFA	Yes

A combination of steel and wooden formwork was constructed to the required beam dimensions. The formwork consisted of a set of three beams, such that all three specimens from a particular group of variables (see **Table 5.2**) would be constructed from the same batch of concrete. Next, the stirrups and longitudinal bars were cut and bent to the required dimensions, and the rebar cages were tied together to the specifications shown in the previous section. Strain gages were installed at both ends of

each splice to monitor the strain in the rebar during testing (**Figure 5.3)**. The cage was then lowered into the forms, using one in. chairs to ensure an adequate clear cover (**Figure 5.4**).

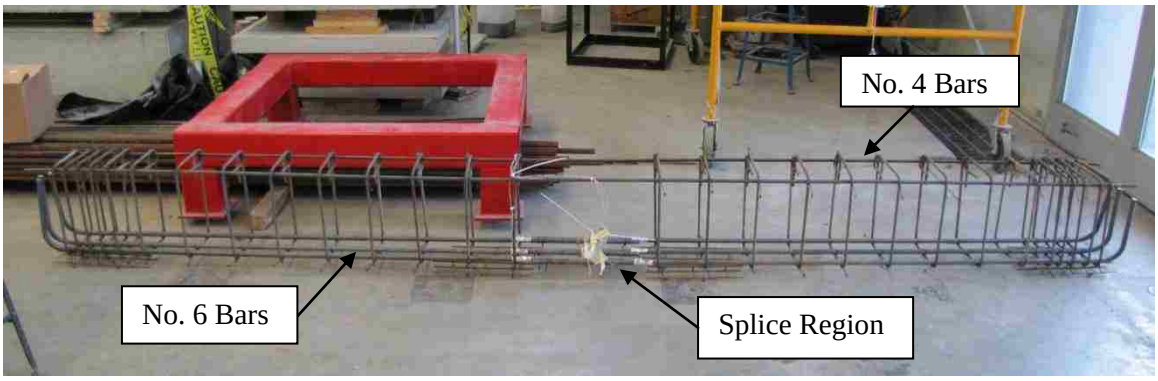

(a) Finished cage viewed from the side

(b) Close up of splice region

Figure 5.3 – Finished cage and close up of spliced bars

Figure 5.4 – Cages in the formwork

Both the control concrete and HVFA concrete were batched from the local ready-mix producer to the specifications detailed in Section 3. For the HVFA concrete, the required amounts of gypsum and calcium hydroxide were added to the ready-mix truck once it arrived at the High-Bay Structures Laboratory (**Figure 5.5**). Once the slump was adjusted to the specified amount through the addition of supplemental water, the concrete was then added to the forms. (Note that approximately 8 to 10 gallons (30 to 38 L) of water was held in abeyance from the ready-mix supplier for this express purpose). A bucket was used to transfer the concrete from the truck to the forms (**Figure 5.6**). Consolidation was achieved using a vibrator, and the tops of the beams were finished with floats and trowels (**Figure 5.7**). Finally, two hours after finishing, the beams were covered with wet burlap and plastic and allowed to cure before being stripped of the forms (three days for the control concrete, one week for the high-volume fly ash concrete). All compressive strength test cylinders were maintained in the exact same curing condition as the beams they represented.

Figure 5.5 – Adding CH and Gypsum to the ready mix truck

Figure 5.6 – Transferring concrete from the truck to the forms using a bucket

Figure 5.7 – Finishing the specimens

5.4. TEST SETUP AND PROCEDURE

5.4.1. Splice Test Setup. A load frame was assembled and equipped with two hydraulic actuators intended to apply the two point loads to the specimens (**Figure 5.8)**. The splice specimens were placed on two roller supports, a foot from each end of the beam, creating a four point loading situation with the two actuators and spreader beam (**Figure 5.9**). The four point loading results in a uniform moment in the splice region, and thus uniform stress, within the splice region. A LVDT was used to measure the deflection of the center of the beam. The strain gages from the beam as well as the LVDT were wired to a data acquisition system where the deflections, strains, and loads were recorded.

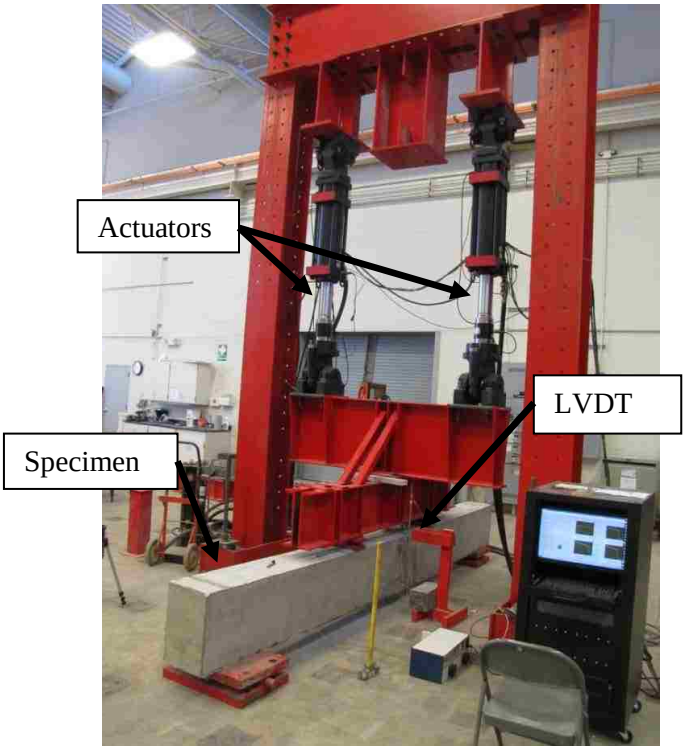

Figure 5.8 – Splice test setup with specimen loaded

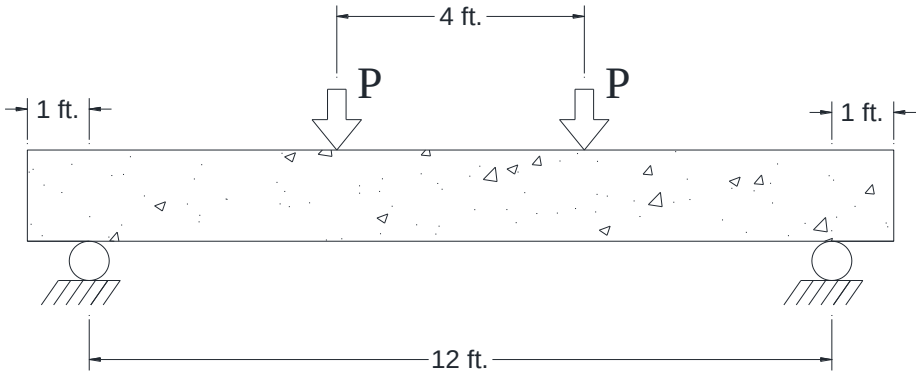

Figure 5.9 – Location of load points on specimen

5.4.2. Splice Test Procedure. The two loads were applied to the beam specimens using an actuator deflection of 0.2 in. (5 mm) per loading cycle, to ensure that a minimum of 10 data points were acquired and to allow periodic surveying of the beam during the test. During the testing, any cracks that formed on the surface of the beam were marked, and the deformation and strains were monitored until the beam failed (**Figure 5.10**).

Figure 5.10 – Failed splice specimen

5.5. RESULTS

Three parameters were recorded for each splice test specimen. These values included applied load (P), rebar strain, and displacement of the beam at the midpoint. **Table 5.3** contains the maximum applied load (P) for each splice specimen and includes the average and coefficient of variation (COV) for each group of specimens. The

theoretical maximum applied load for each splice specimen assuming yielding of the bars instead of a bond failure is also shown in the table, which indicates that all of the splice specimens experienced a premature bond failure – the intended result. A statistical analysis of the test data is available in Appendix D. According to the t-test, the data averages for both specimen types are statistically identical. **Figures 5.11** through **5.14** are photographs of the failed test specimens within the splice region. Each specimen displays horizontal cracking consistent with a bond failure.

Table 5.3 – Beam splice test results

Specimen	Max Theoretical P (kips)	Max Applied P (kips)	Average Applied P (kips)	COV (%)
Cont-NC-1	31	26.67	27.38	2.4
Cont-NC-2		28.00		
Cont-NC-3		27.47		
FA-NC-1	31	23.63	24.44	4.6
FA-NC-2		23.96		
FA-NC-3		25.72		
Cont-C-1	30	28.11	28.54	5.5
Cont-C-2		27.21		
Cont-C-3		30.29		
FA-C-1	30	27.49	25.75	5.9
FA-C-2		24.69		
FA-C-3		25.08		

(1 kip = 4.45 kN)

Figure 5.11 – Failed control specimen with no confinement

Figure 5.12 – Failed control specimen with confinement

Figure 5.13 – Failed fly ash specimen with no confinement

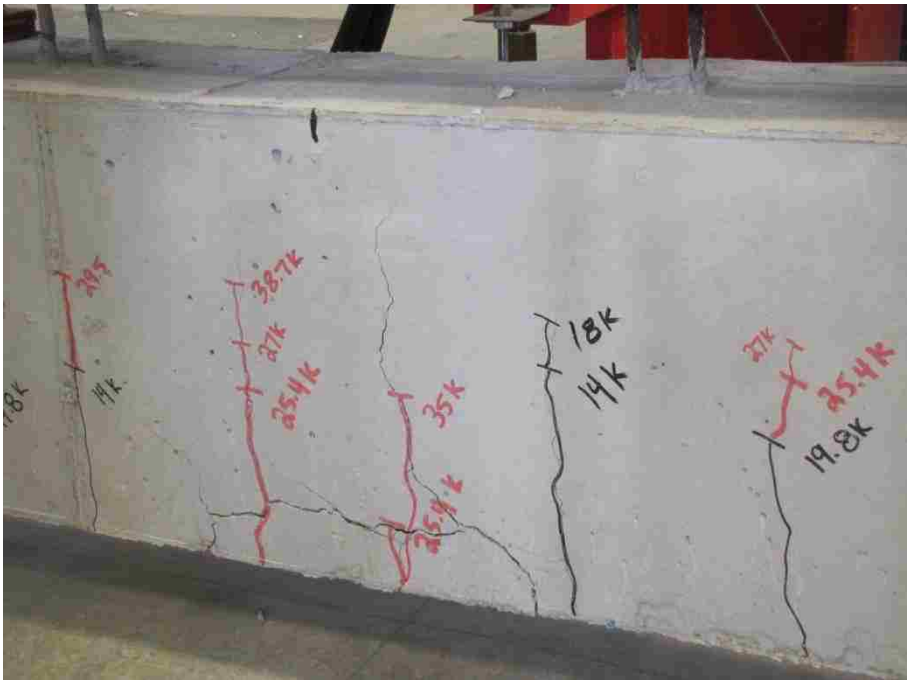

Figure 5.14 – Failed fly ash specimen with confinement

Table 5.4 contains the compressive strength test data for each concrete pour and includes the average and COV for each group of specimens.

Table 5.4 – Compressive strength test data

	Test Day Strength (psi)				
	Cylinder 1	**Cylinder 2**	**Cylinder 3**	**Average**	**COV**
Cont-NC	6560	7435	7790	7262	8.7%
Cont-C	7127	6735	7074	6979	3.1%
FA- NC	4841	4682	4968	4830	3.0%
FA- C	4386	4137	4748	4424	7.0%

(1 psi = 6.89 kPa)

The data was also organized into plots of load vs. displacement and load vs. strain. An example plot of load vs. displacement is shown in **Figure 5.15** for Specimen FA-NC-1, which corresponds to a specimen constructed with fly ash concrete (FA) with no confinement (NC) steel within the splice region. As shown in the plot, there are two distinct linear portions of the response. The first occurs from a load of 0 to a load of approximately 4 kips (18 kN). The second occurs from a load of approximately 4 kips (18 kN) until failure at 23.64 kips (105 kN). The shift in slope at around 4 kips (18 kN) is likely due to cracking of the concrete in tension. More importantly, the linear portion of the load-deflection plot up until failure is also indicative of a premature bond failure – the intended result.

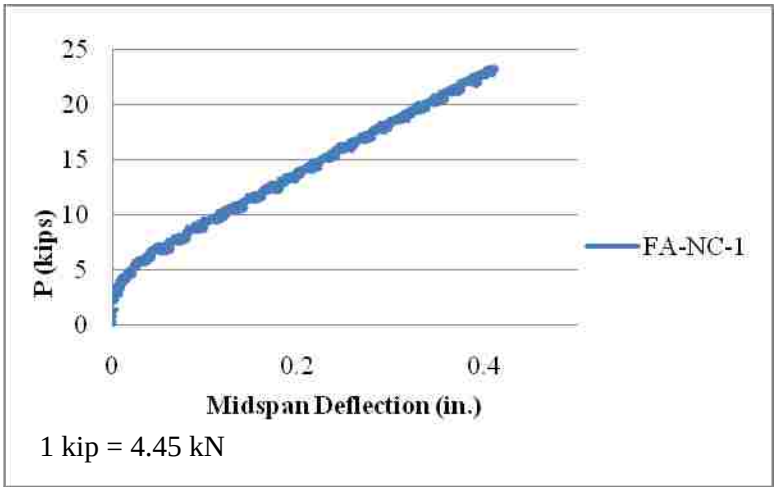

Figure 5.15 – Displacement vs. load plot for specimen FA_NC-1

An example plot of load vs. strain is shown in **Figure 5.16** for Specimen FA-NC-1, which is the same specimen as plotted in **Figure 5.15**. As shown in the plot, there are also two distinct linear portions of the response. The first occurs from a load of 0 to a load of approximately 4 kips (18 kN). The second occurs from a load of approximately 4 kips (18 kN) until failure at 23.64 kips (105 kN). The shift in slope likely occurs due to flexural cracking. Again, more importantly, the linear portion of the load-strain plot up until failure is also indicative of a premature bond failure – the intended result.

Similar plots for all of the bond test specimens follow the same general patterns. The complete data for each individual test is included in **Appendix A (Table A.2).**

5.6. DATA ANALYSIS AND INTERPRETATION

5.6.1. Failure Load Analysis. Figure 5.17 is a plot of the average failure load for each specimen group and includes an error bar representing one standard deviation above and below the average value. As shown in the figure, and in **Table 5.2**, the test

results were extremely consistent, with a typical COV of only 5 percent. Also note that the results for the confined splice are slightly higher in all instances, which was to be expected.

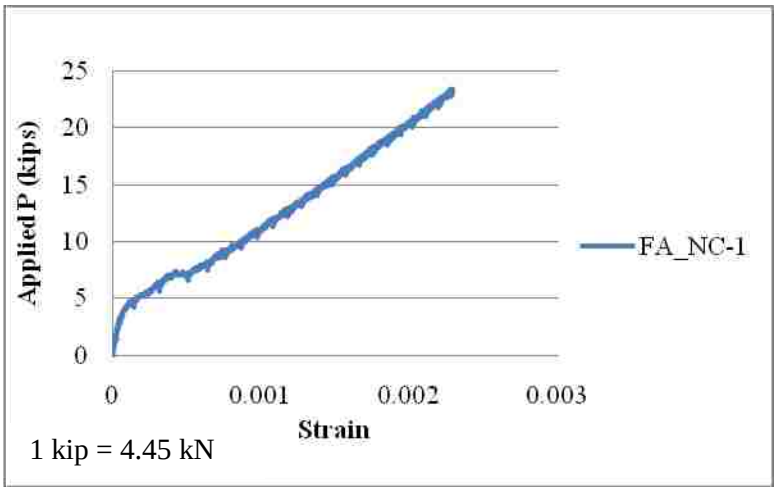

Figure 5.16 – Load vs. strain plot for specimen FA_NC-1

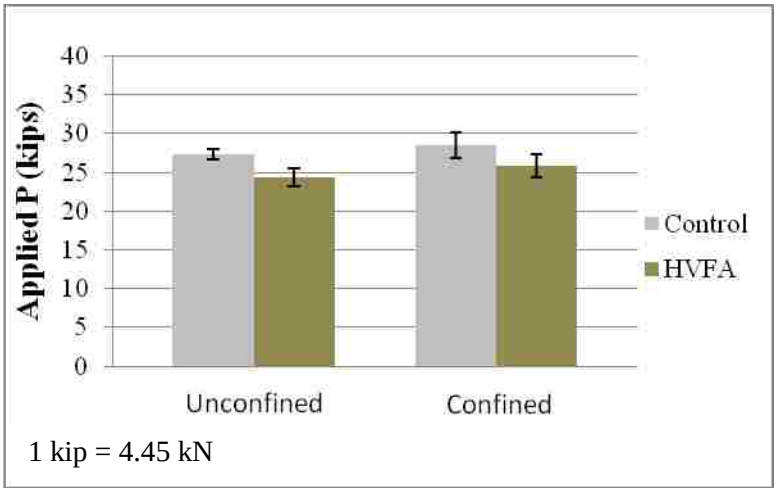

Figure 5.17 – Average failure load for each specimen type

However, when comparing the test data of the HVFA concrete with the control concrete, it is necessary to adjust the results to reflect the different compressive strengths of the specimens. As mentioned previously, the development length equation in ACI 318 (2008), repeated below, is a function of a number of variables that represent the specific characteristics of a given situation. However, for the splice test specimens, all of these variables were identical except for concrete strength. Therefore, to normalize the data for comparison, the failure loads were divided by the square root of compressive strength (**Table 5.5)** and replotted in **Figure 5.18**. These results indicate that the HVFA beam specimens were able to support a higher modified applied load than the control beams before the splice failed, therefore exhibiting a stronger bond between the HVFA concrete and the reinforcing bars.

$$l_d = \left(\frac{3}{40} \frac{f_y}{\lambda \sqrt{f'_c}} \frac{\psi_t \psi_e \psi_s}{\left(c_b + \frac{K_{tr}}{d_b} \right)} \right) d_b \qquad (5.1)$$

where:

l_d = development length

f_y = specified yield strength of reinforcement

λ = light weight concrete modification factor

f'_c = specified compressive strength of concrete

ψ_t = reinforcement location modification factor

ψ_e = reinforcement coating modification factor

ψ_s = reinforcement size modification factor

c_b = the smaller of: the distance from the centroid of a bar to the nearest concrete

surface and the center to center spacing of bars being developed.

K_{tr} = transverse reinforcement index

d_b = bar diameter

Table 5.5 - Pull-out test results with modified loads

Specimen	Max Applied P (kip)	Concrete Compressive Strength (ksi)	Modified P (lb/√psi)	Average Modified P (lb/√psi)	COV (%)
Cont-NC-1	26.67	7262	312.97	321.3	2.4
Cont-NC-2	28.00		328.58		
Cont-NC-3	27.47		322.36		
FA-NC-1	23.63	4830	340.00	351.6	4.6
FA-NC-2	23.96		344.75		
FA-NC-3	25.72		370.07		
Cont-C-1	28.11	6979	336.49	341.6	5.5
Cont-C-2	27.21		325.72		
Cont-C-3	30.29		362.59		
FA-C-1	27.49	4424	413.32	387.2	5.9
FA-C-2	24.69		371.22		
FA-C-3	25.08		377.08		

(1 kip = 4.45 kN, 1 ksi = 6.89 MPa, 1 lb/√psi = 8.36 N/√Pa)

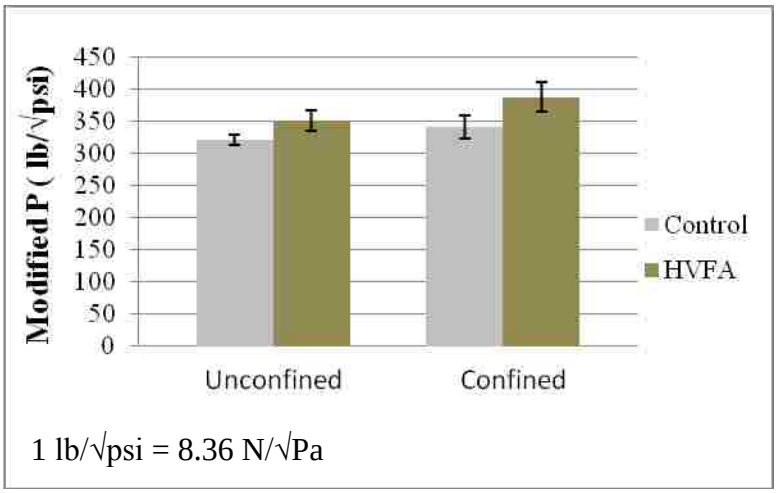

1 lb/√psi = 8.36 N/√Pa

Figure 5.18 – Splice specimen load comparisons (average)

5.6.2. Strain Analysis. The majority of the strain data collected from each beam was graphed in a load vs. strain format. These results were then compared to strain data acquired from rebar tensile specimens described in Section 5.2. According to this data, each splice specimen failed before the maximum experimental strain (determined from the tensile tests) was reached in the rebar. This result indicates that each specimen ultimately failed due to the bond around the splices failing and not from the rebar itself. A typical modified load vs. strain relationship was plotted for both a control specimen and a HVFA specimen (both with confinement) and presented side by side in **Figure 5.19.** According to the plot, both specimens displayed very similar behavior during testing. The only difference is the number of times the control specimen experienced a slope change where as the plot for the HVFA specimen was smoother throughout the course of testing. This behavior for the control specimen, as mentioned above, can be attributed to flexure cracking during the different phases of testing.

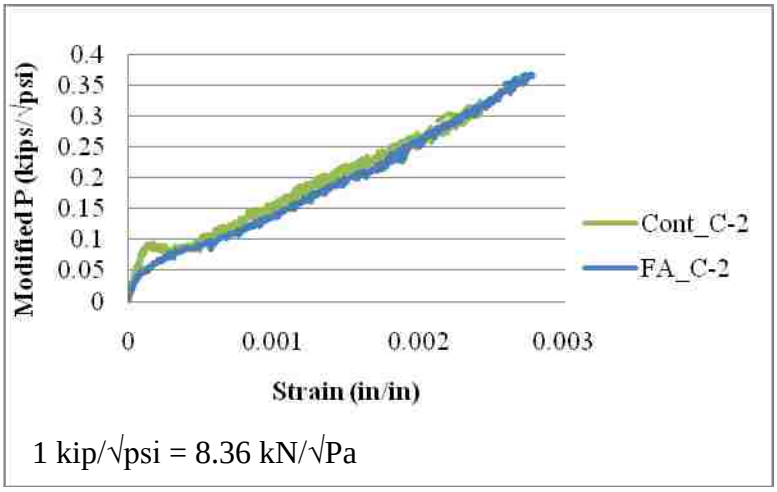

Figure 5.19 – Load vs. strain plot

5.7. CONCLUSIONS

The load data collected from the splice tests, once modified for the specimen compressive strengths, indicates that the high-volume fly ash concrete specimens were able to support more load before the splice failed than the control specimens. These findings, along with the findings from the pull-out tests, indicate that the use of high volumes of fly ash as a cement substitute is not only feasible in terms of bond, but also superior in some cases.

6. FINDINGS, CONCLUSIONS, AND RECOMMENDATIONS

Currently, high-volume fly ash (HVFA) concrete is used mostly for ornamentation and various non load bearing applications. Few structures have been built utilizing this less proven material. The ***objective*** of this study was to explore the effects of substituting large amounts of fly ash on the concrete to reinforcement bond strength, which, ultimately, along with other strength and durability tests (Marlay, 2011) examined the feasibility of using HVFA concrete for the sustained construction of structures.

This section contains the findings from the mix development, pull-out tests, and beam splice tests. Next, the conclusions based on these findings are presented along with recommendations for future research.

6.1. FINDINGS

The findings from the mix development as well as the pull-out testing and beam splice testing were recorded and divided into the following sections.

6.1.1. Mix Development. The mix development phase of this study was used to find a plausible HVFA concrete mix and control mix for the pull-out testing and beam splice testing. Listed below are the findings that led to the mixes chosen for this study:

- A lower water-to-cementitious ratio of 0.40 can be used for a HVFA mix
- The use of activators such as calcium hydroxide and gypsum increased the early compressive strengths for HVFA concrete mixes

- Mix designs using 50, 60, and 70 percent cement replacement with fly ash, and added calcium hydroxide and gypsum , yielded early age compressive strengths as well as 28 day strengths acceptable for construction.
- The 70 percent fly ash mix (with 4 percent gypsum and 10 percent calcium hydroxide) was the highest percent fly ash mix to still have sufficient compressive strengths.

6.1.2. Pull-out Testing. The pull-out tests were performed on 6 specimens of each mix, 3 per mix using a No. 4 bar and the other 3 per mix using a No. 6 bar. Each specimen was tested until failure and the findings from these tests are listed below:

- All specimens failed due to pull-out (localized concrete crushing)
- HVFA concrete specimens failed at loads similar to those of the control specimens once adjusted for the respective compressive strengths
- Slip initially occurred at similar loads for both the HVFA concrete and control specimens
- Once initial slip occurred for both concrete mixes, the load fell much faster for the HVFA concrete specimens than for the control specimens

6.1.3. Beam Splice Testing. The beam splice tests were performed on a series of beams with confinement present in the splice zone as well as no confinement present in the splice zone for both mix types. The findings from the beam splice tests are listed below:

- All specimens failed at the splice
- Steel reinforcement did not yield for any test

- Behavior at failure was more violent for specimens with no splice confinement (consistent with past research)
- Once the load (P) was modified for concrete strength, the HVFA concrete specimens outperformed the control specimens

6.2 CONCLUSIONS

Based on the previously listed findings for each test performed for this study, the following conclusions were drawn that support the validity of bond strength for HVFA concrete mixes.

6.2.1. Mix Development. Based on the findings from the compression cube and compression cylinder testing performed as a part of the mix development phase of research, the optimal mix designs for the HVFA and control specimens were determined based on the reactivity of the provided fly ash. The mix selected for the experimental HVFA concrete specimens was the 70 percent fly ash mix (w/cm = 0.40), with 4 percent gypsum, and 10 percent calcium hydroxide.

6.2.2. Pull-out Testing. The data recorded from the pull-out tests supports the effectiveness of HVFA concrete in terms of bond integrity. Since the pull-out test is a comparative test, this conclusion can be drawn based on the fact that the HVFA specimens demonstrated similar bond strengths to the control specimens (based on maximum modified load applied). The only drawback for the HVFA concrete was that once the concrete began to crush around the reinforcing bar, slip occurred at a higher rate for the HVFA specimens.

6.2.3. Beam Splice Testing. The load data collected from the splice tests, once modified for the specimen compressive strengths, indicates that the high-volume fly ash concrete specimens were able to support more load before the splice failed than the control specimens. These findings, along with the findings from the pull-out tests, indicate that the use of high volumes of fly ash as a cement substitute is not only feasible in terms of bond, but also superior in some cases.

6.3. RECOMMENDATIONS

Future research opportunities are available for the bond behavior of HVFA concrete simply because it is a topic that has seldom been researched in the past. Much more research must be performed in order to build up a data base of results that can eventually be used for comparison as well as for future ACI design codes. Also important for design would be to explore whether or not certain ACI code distinctions, such as confinement or bar size factors, for classic concrete designs also apply to HVFA concrete, or if they need to be tailored specifically to HVFA concrete. Below is a list of recommendations for testable variables related to this topic:

- Perform tests with a larger variation of bar sizes based on ACI 318 code distinctions for bar size effect on development length
- Through design, induce different failure modes such as splitting for pull-out tests
- Cast beam splice specimens upside down to test the top bar effect (ψ_t from the ACI 318 code)

- Perform tests with fly ash from different sources
- Perform tests with aggregates from different sources
- Perform bond tests on more specimen types mentioned in ACI

APPENDIX A

PULL-OUT AND SPLICE TEST DATA TABLES

Table A.1 – Test day compressive strengths for pull-out specimens

	Test Day Strength (psi)				
	Cylinder 1	**Cylinder 2**	**Cylinder 3**	**Average**	**COV (%)**
All FAPO	4386	4137	4748	4424	0.07
All CPO	5662	5905	5718	5762	0.02

(1 psi = 6.89 kPa)

Table A.2 – Pull-out test results

Specimen	**Max Applied Load (lb)**	**Concrete Compressive Strength (psi)**	**Modified Load (lb/√(f'c)**	**Average Modified Load (lb/√(f'c)**	**CV (Modified Load) (%)**
CPO_4-1	11994	5762	158	156	2.6
CPO_4-2	11989		158		
CPO_4-3	11469		151		
FAPO_4-1	10830	4424	163	167	2.0
FAPO_4-2	11183		168		
FAPO_4-3	11225		169		
CPO_6-1	32099	5762	423	430	1.4
CPO_6-2	32854		433		
CPO_6-3	32920		434		
FAPO_6-1	28471	4424	428	410	4.3
FAPO_6-2	27154		408		
FAPO_6-3	26119		393		

(1 lb = 4.45 N, 1 psi = 6.89 kPa, 1 lb/√(psi) = 8.36 N/√(Pa))

Table A.3 – Test day compressive strengths for beam splice specimens

	Test Day Strength (psi)				
	Cylinder 1	**Cylinder 2**	**Cylinder 3**	**Average**	**COV (%)**
Cont-NC	6560	7435	7790	7262	8.7
Cont-C	7127	6735	7074	6979	3.1
FA-NC	4841	4682	4968	4830	3.0
FA-C	4386	4137	4748	4424	7.0

(1 psi = 6.89 kPa)

Table A.4 – Beams splice test results

Specimen	Max Applied P (kip)	Concrete Compressive Strength (ksi)	Modified P (lb/√psi)	Average Modified P (lb/√psi)	COV (Modified P) (%)
Cont-NC-1	26.67	7262	312.97	321.30	2.4
Cont-NC-2	28.00		328.58		
Cont-NC-3	27.47		322.36		
FA-NC-1	23.63	4830	340.00	351.60	4.6
FA-NC-2	23.96		344.75		
FA-NC-3	25.72		370.07		
Cont-C-1	28.11	6979	336.49	341.60	5.5
Cont-C-2	27.21		325.72		
Cont-C-3	30.29		362.59		
FA-C-1	27.49	4424	413.32	387.21	5.9
FA-C-2	24.69		371.22		
FA-C-3	25.08		377.08		

(1 lb = 4.45 N, 1 psi = 6.89 kPa, 1 lb/√(psi) = 8.36 N/√(Pa))

Table A.5 – 28 day compressive strengths for pull-out specimens

	28 Day Strength (psi)			
	Cylinder 1	**Cylinder 2**	**Cylinder 3**	**Average**
All FAPO	4415	4257	4019	4230
All CPO	6396	5613	4980	5663

(1 psi = 6.89 kPa)

Table A.6 – 28 day compressive strengths for beam splice specimens

	28 Day Strength (psi)			
	Cylinder 1	**Cylinder 2**	**Cylinder 3**	**Average**
Cont-NC	6396	5613	4980	5663
Cont-C	6412	5993	6126	6177
FA-NC	4905	4652	4869	4809
FA-C	4415	4257	4019	4230

(1 psi = 6.89 kPa)

APPENDIX B

PULL-OUT AND SPLICE TEST DATA PLOTS

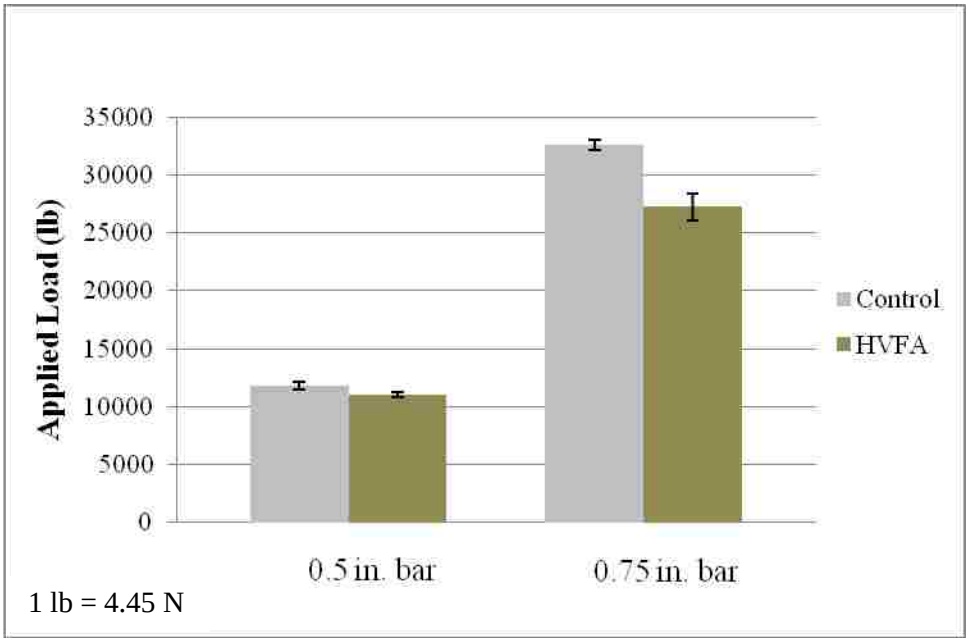

Figure B.1 - Pull-out applied load comparisons

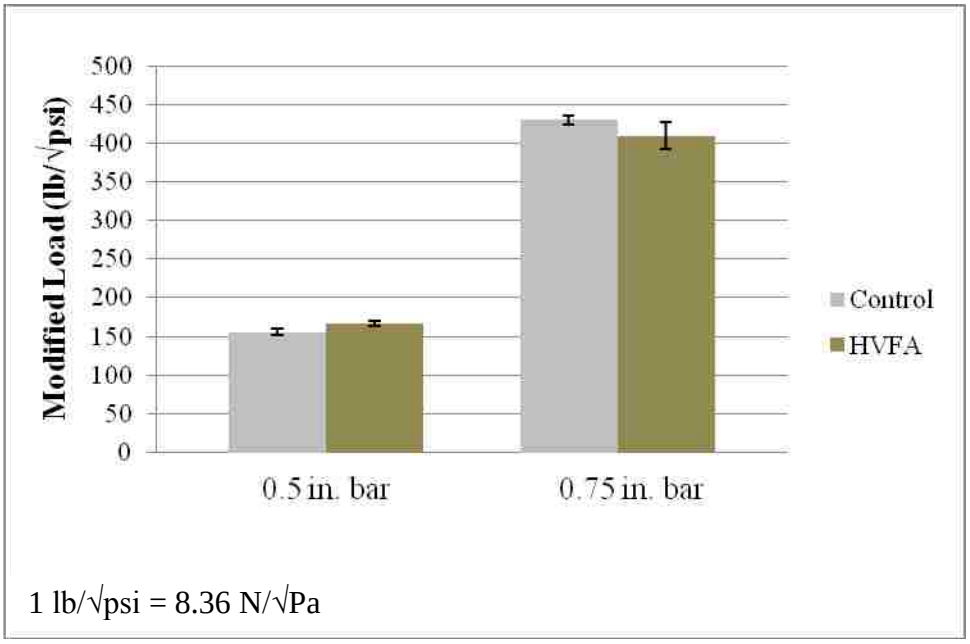

Figure B.2 - Pull-out modified load comparisons

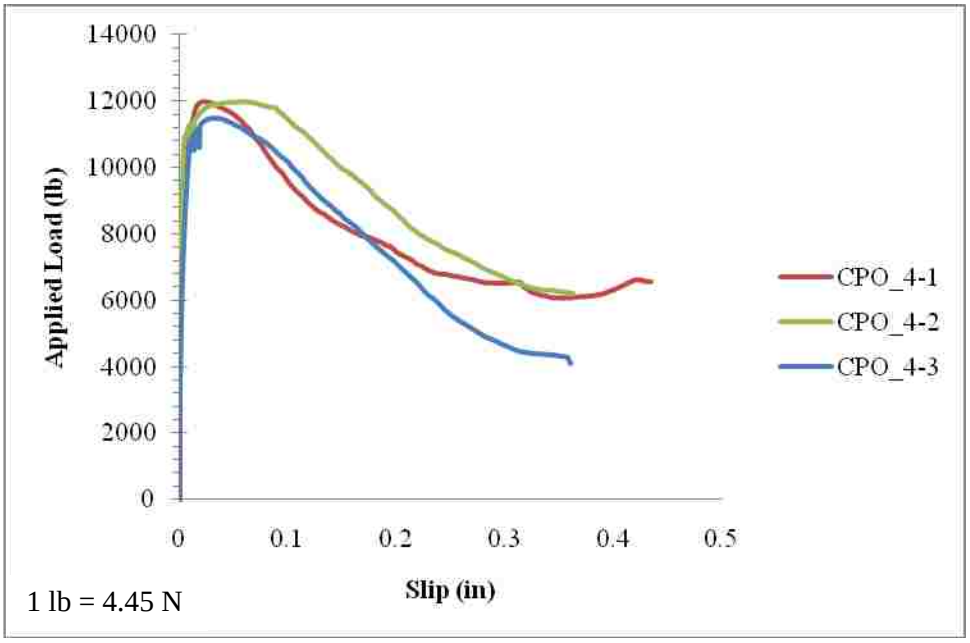

Figure B.3 – Applied load vs. slip plot for CPO_4 specimens

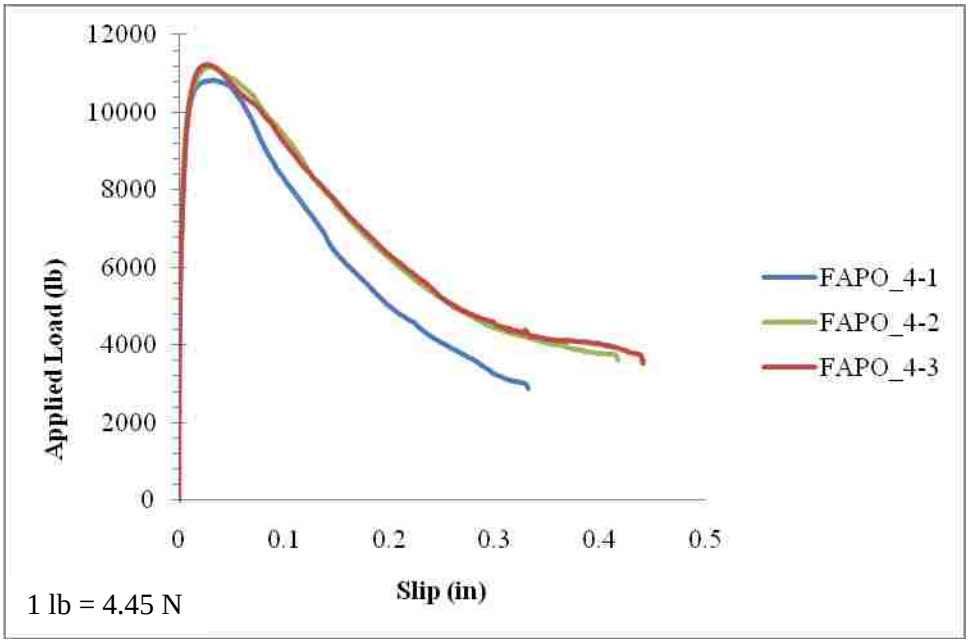

Figure B.4 – Applied load vs. slip plot for FAPO_4 specimens

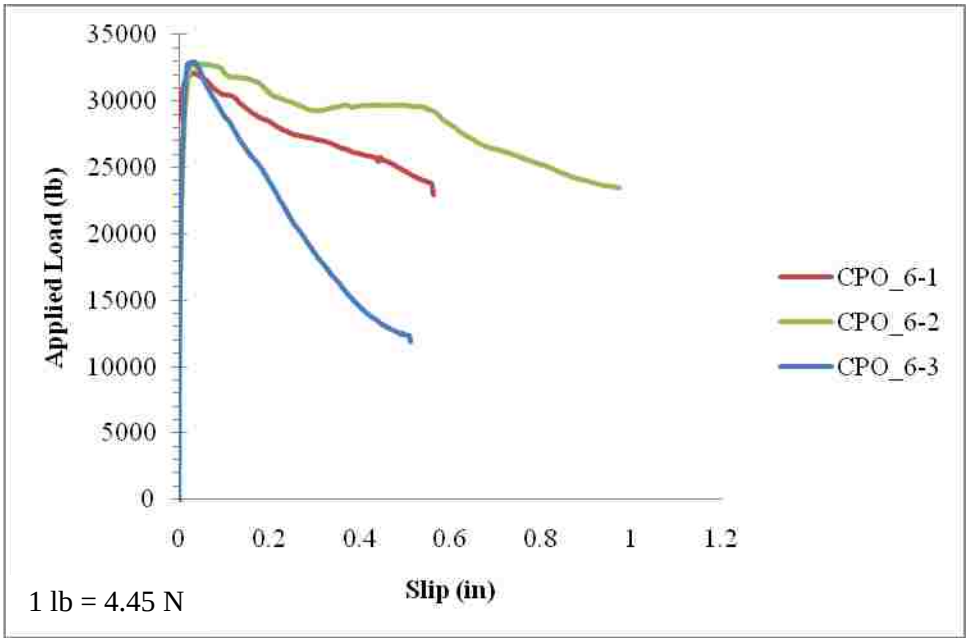

Figure B.5 – Applied load vs. slip plot for CPO_6 specimens

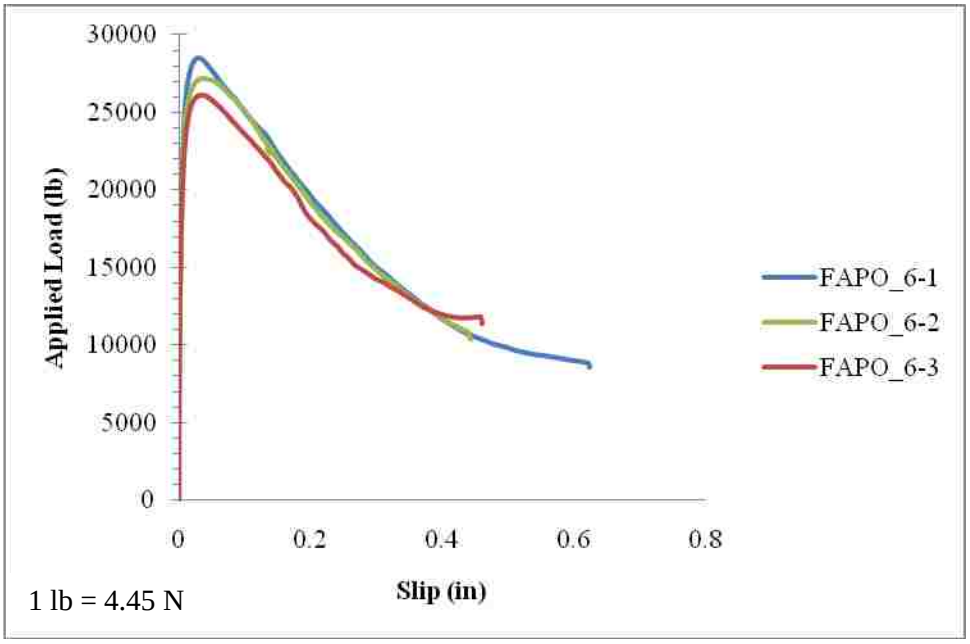

Figure B.6 – Applied load vs. slip plot for FAPO_6 specimens

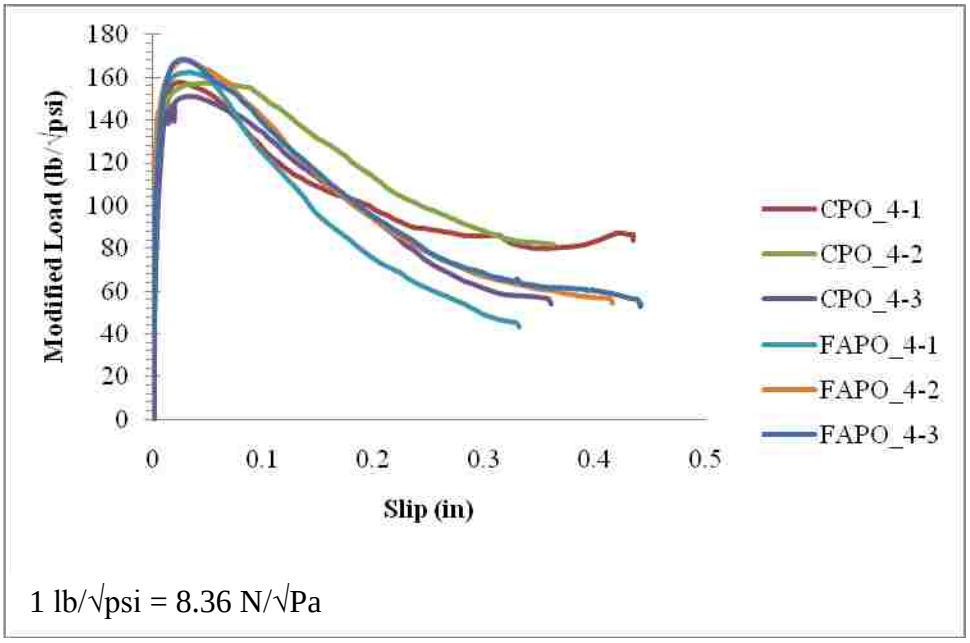

Figure B.7 – Modified load vs. slip for all pull-out specimens with No. 4 bars

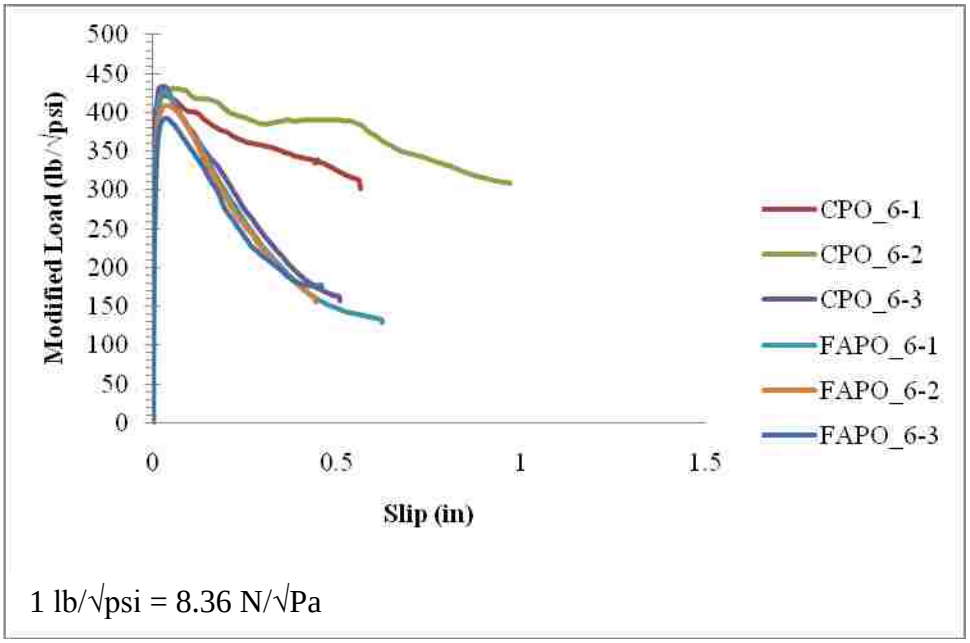

Figure B.8 – Modified Load vs. slip for all pull-out specimens with No. 6 bars

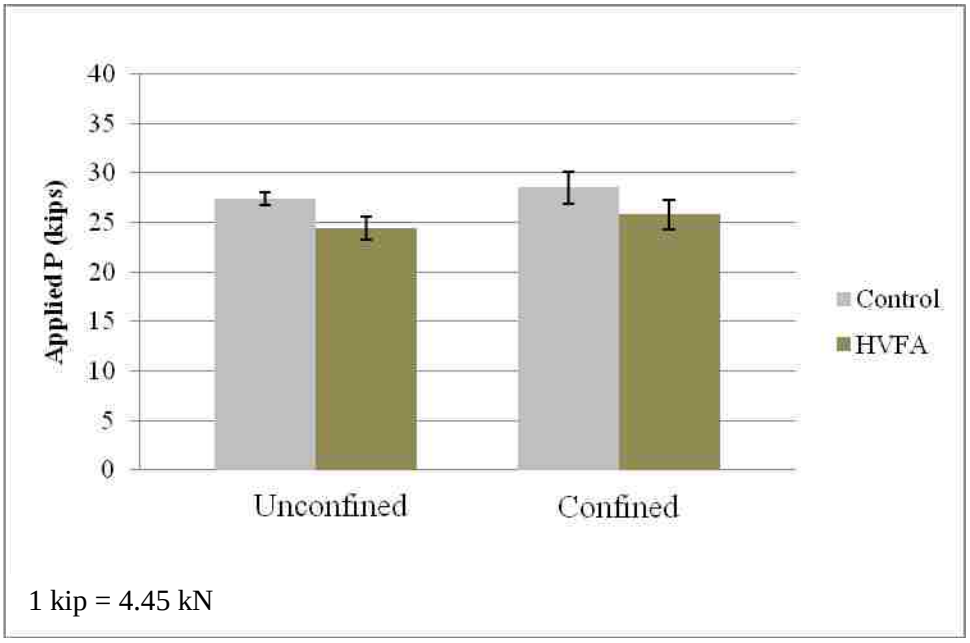

Figure B.9- Beam splice applied load comparisons

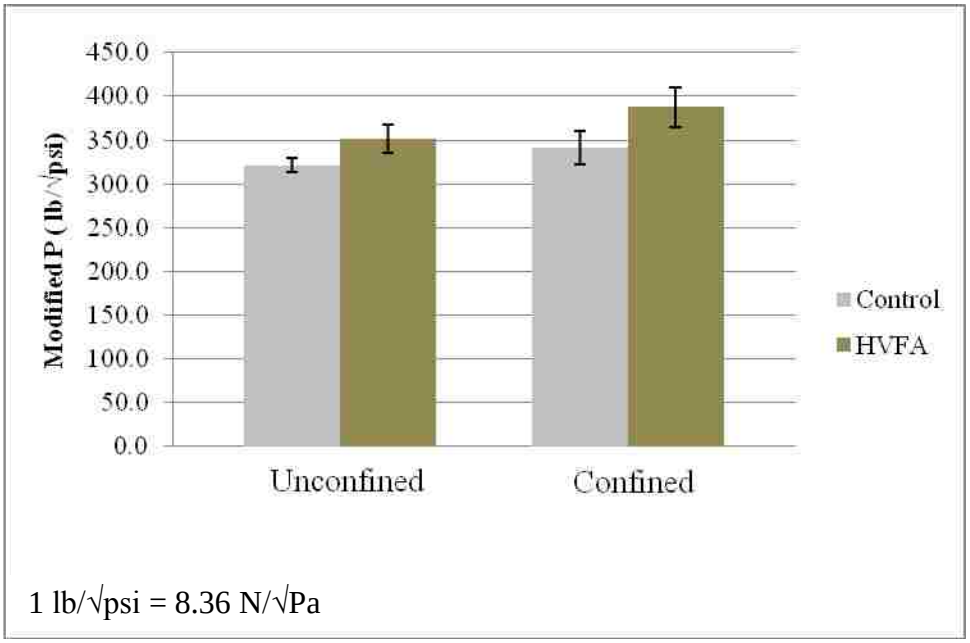

Figure B.10- Beam splice modified load comparisons

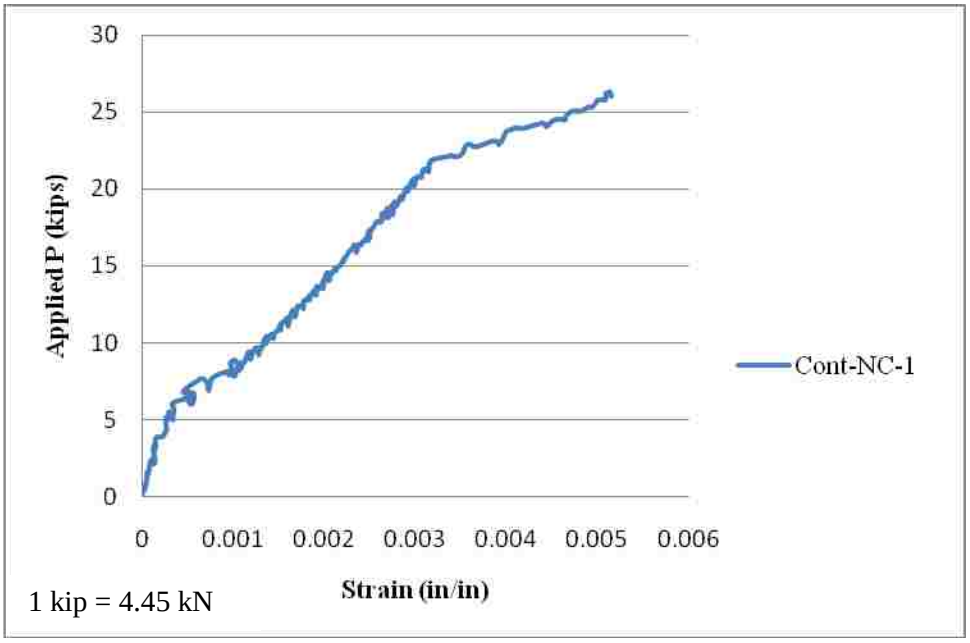

Figure B.11 – Applied P vs. strain (average of all gages per specimen) for Cont_NC

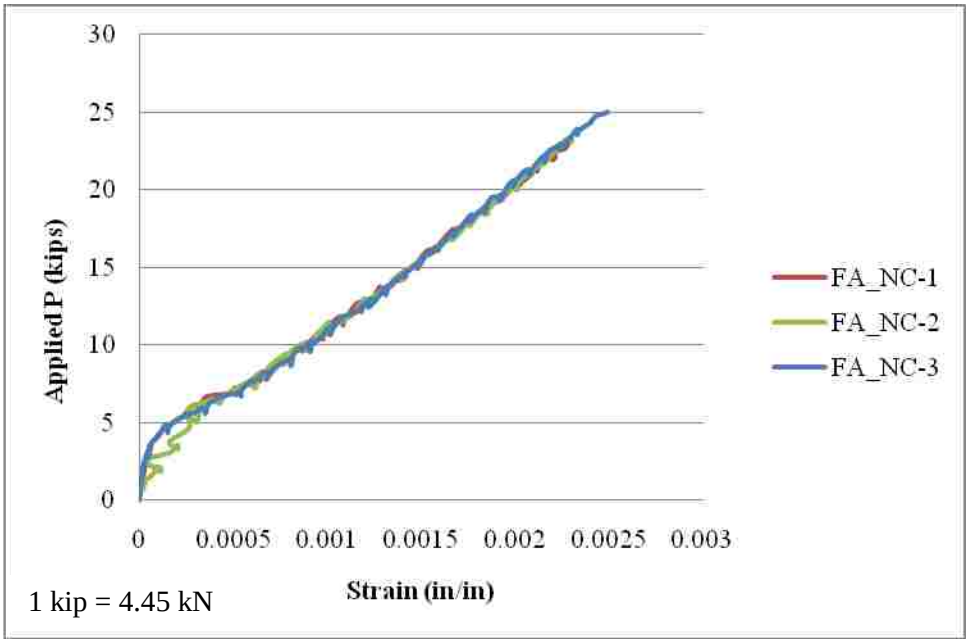

Figure B.12 – Applied P vs. strain (average of all gages per specimen) for FA_NC

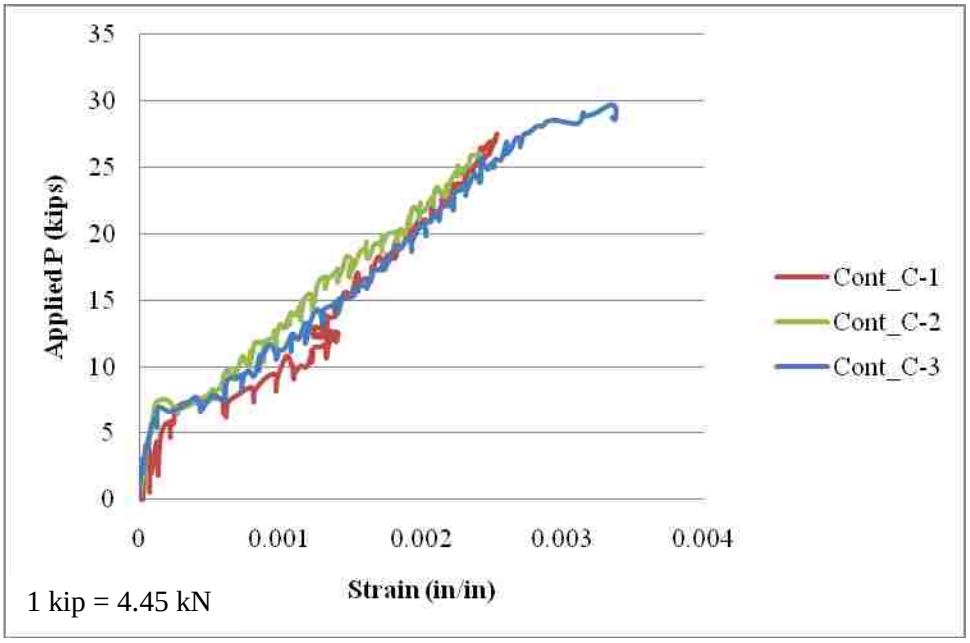

Figure B.13 – Applied P vs. strain (average of all gages per specimen) for Cont_C

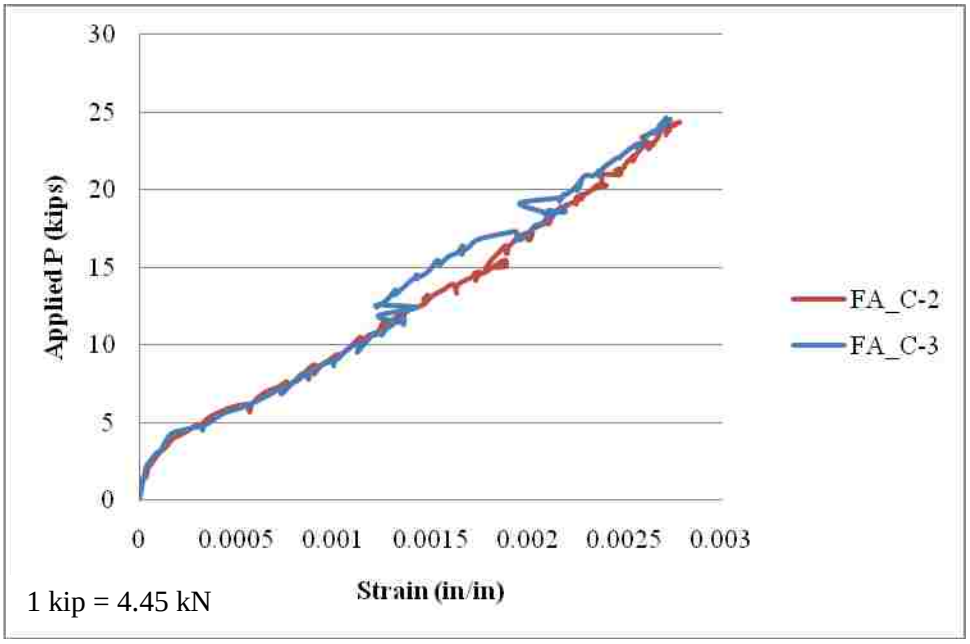

Figure B.14 – Applied P vs. strain (average of all gages per specimen) for FA_C

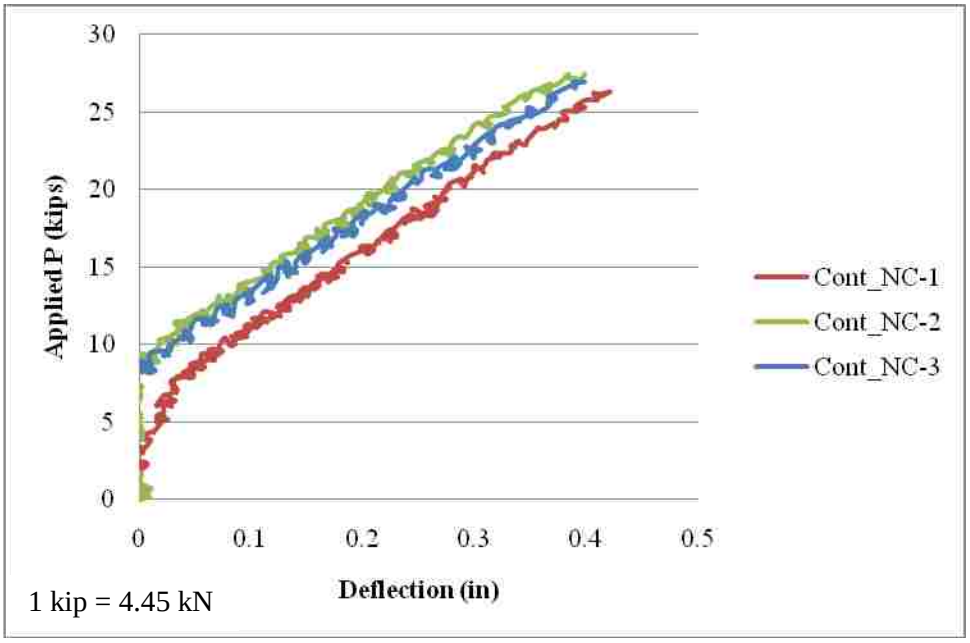

Figure B.15 – Applied load (P) vs. displacement for Cont_NC

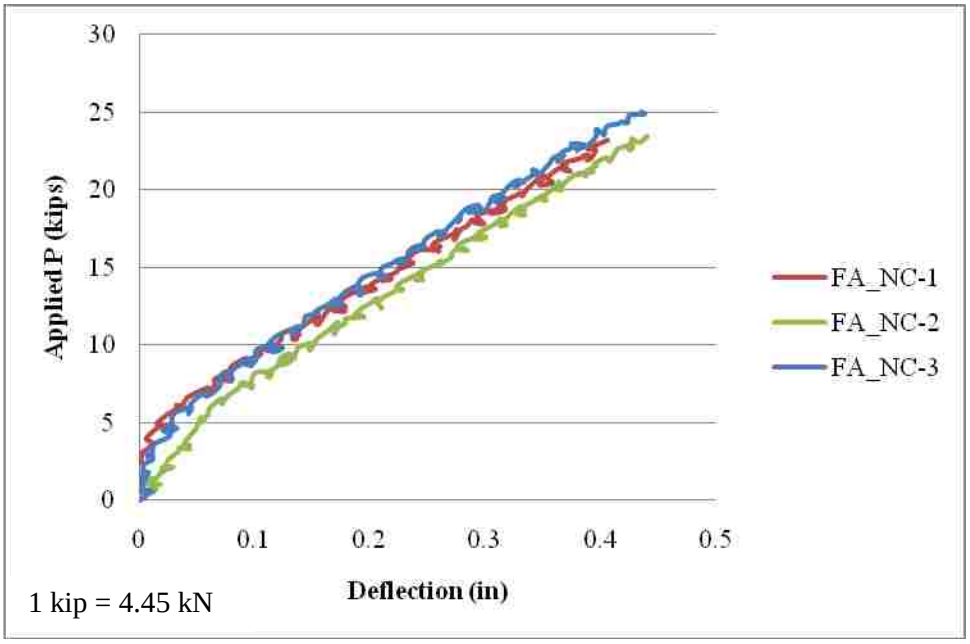

Figure B.16 – Applied load (P) vs. displacement for FA_NC

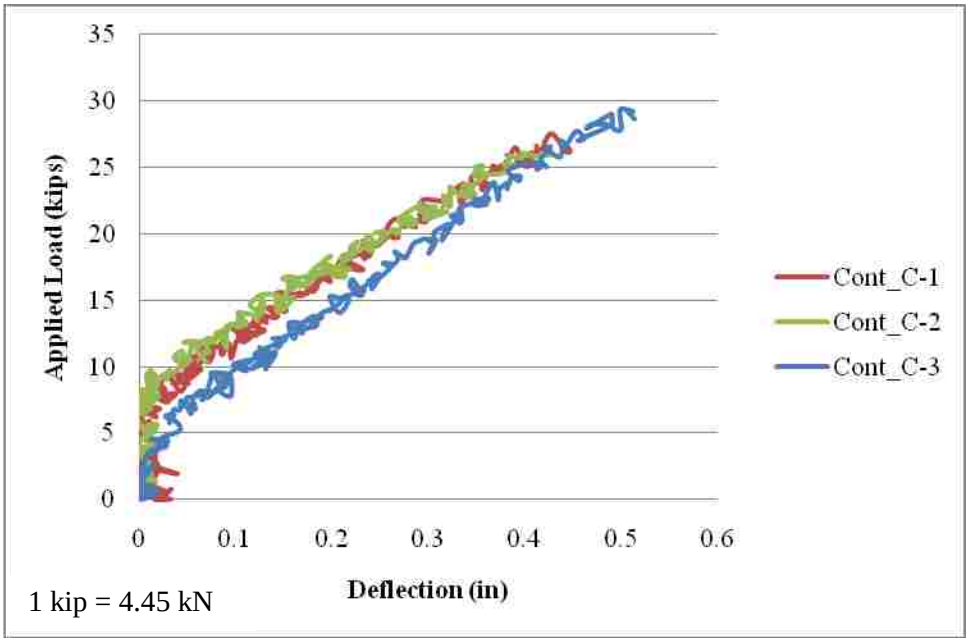

Figure B.17 – Applied load (P) vs. displacement for Cont_C

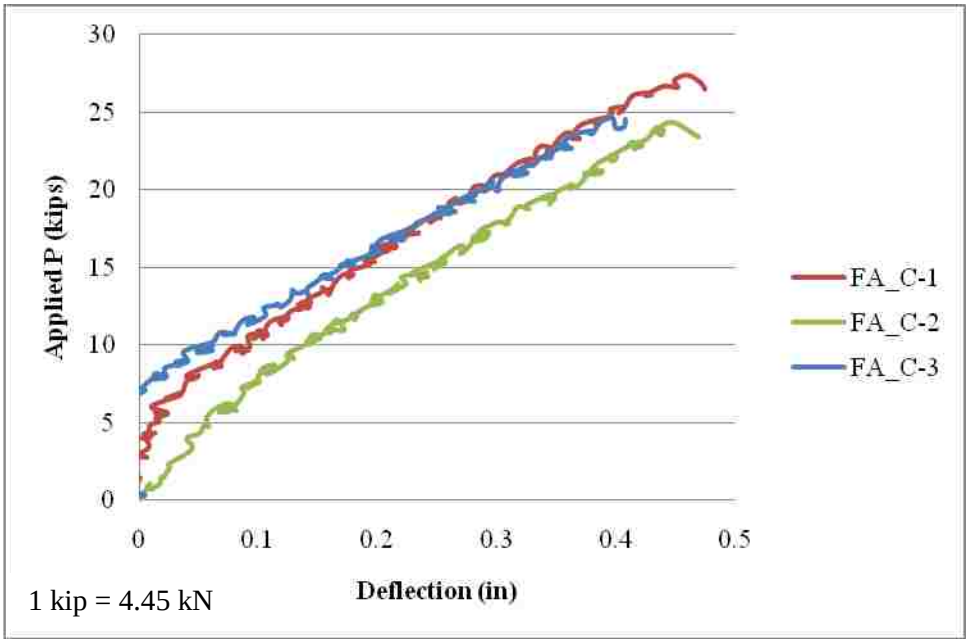

Figure B.18 – Applied load (P) vs. displacement for FA_C

APPENDIX C

MATERIALS TABLES AND PLOTS

Table C.1 – Chemical Analysis of Ameren UE fly ash

Oxide	*%*
Silicon Oxide (SiO_2)	30.45 – 36.42
Aluminum Oxide (Al_2O_3)	16.4 – 20.79
Iron Oxide (Fe_2O_3)	6.78 – 7.73
Calcium Oxide (CaO)	24.29 – 26.10
Magnesium Oxide (MgO)	4.87 – 5.53
Sulfur (SO_3)	2.18 – 6.36
Sodium Oxide (Na_2O)	1.54 – 1.98
Potassium Oxide (K_2O)	0.38 – 0.57
Titanium Oxide (TiO_2)	1.42 – 1.56
Phosphorus Oxide (P_2O_5)	1.01 – 1.93
Manganese Oxide (MnO)	0.028 – 0.036
Strontium Oxide (SrO)	0.40 – 0.44
Barium Oxide (BaO)	0.68 – 0.99
LOI	0.24 – 1.15

Table C.2 – Fly ash chemical differences expressed as percent by weight

Component	Bituminous	Sub-bituminous	Lignite
SiO_2	20 – 60	40 – 60	15 – 45
Al_2O_3	5 – 35	20 – 30	10 – 25
Fe_2O_3	10 – 40	4 – 10	4 – 15
CaO	1 – 12	5 – 30	15 – 40
MgO	0 – 5	1 – 6	3 – 10
SO_3	0 – 4	0 – 2	0 – 10
Na_2O	0 – 4	0 – 2	0 – 6
K_2O	0 – 3	0 – 4	0 – 4
LOI	0 – 15	0 – 3	0 – 5

Table C.3 – Test matrix for mortar cubes

		% of Cementitious Material	
Specimen Set *	**w/cm**	**Cement**	**Fly Ash**
Control-0.40	0.4	100	0
50/50-0.40		50	50
25/75-0.40		25	75
100% FA-0.40		0	100
Control-0.30	0.3	100	0
50/50-0.30		50	50
25/75-0.30		25	75
100% FA-0.30		0	100

*Each set is comprised of the average of three specimens

Table C.4 – Test matrix for paste cubes

	% of Cementitious Material			
Specimen Set *	**Cement**	**Fly Ash**	**Gypsum**	**Calcium Hydroxide**
Control	100	0	-	-
50/50	50	50	-	-
40/60	40	60	-	-
25/75	25	75	-	-
100% FA	0	100	-	-
50/50-G	50	50	4	-
40/60-G	40	60	4	-
25/75-G	25	75	4	-
100% FA-G	0	100	4	-
50/50-G-10CH	50	50	4	10
40/60-G-10CH	40	60	4	10
25/75-G-10CH	25	75	4	10
100% FA-G-10CH	0	100	4	10
50/50-G-15CH	50	50	4	15
40/60-G-15CH	40	60	4	15
25/75-G-15CH	25	75	4	15
100% FA-G-15CH	0	100	4	15

*Each set is comprised of the average of three specimens

Table C.5 – Compressive strengths for mortar cubes

		Compressive Strength (psi)		
Specimen Set	**w/cm**	**Day 3**	**Day 7**	**Day 28**
Control-0.40	0.40	3435	5275	5506
50/50-0.40		2726	4079	5368
25/75-0.40		1003	1906	2909
100% FA-0.40		74	313	520
Control-0.30	0.30	2905	4695	5105
50/50-0.30		2106	2176	3926
25/75-0.30		1434	1824	2384
100% FA-0.30		218	468	881

(1 psi = 6.89 kPa)

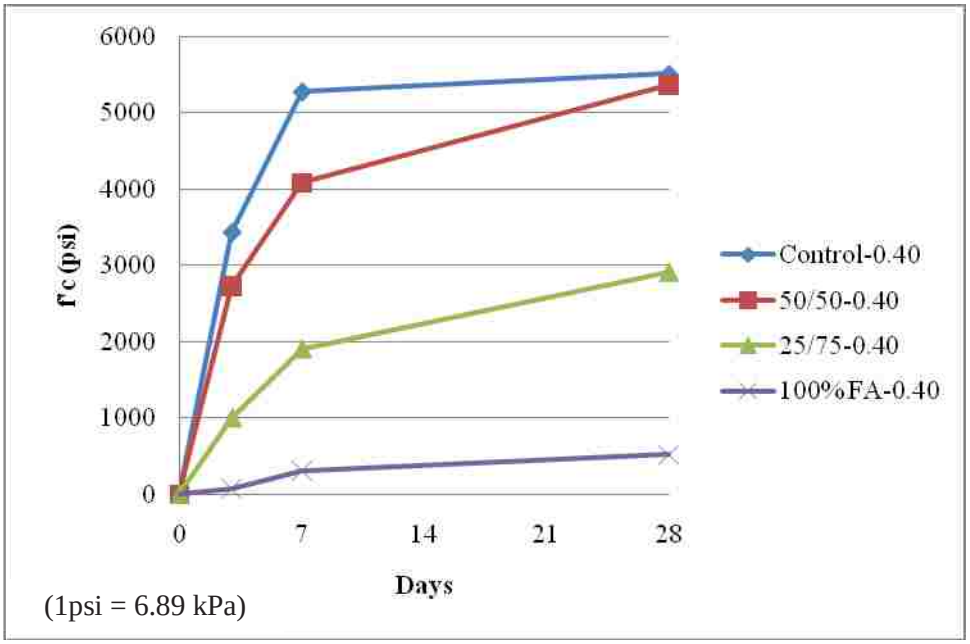

Figure C.1 – Mortar cube compressive strengths on test days (*w/cm* = 0.40)

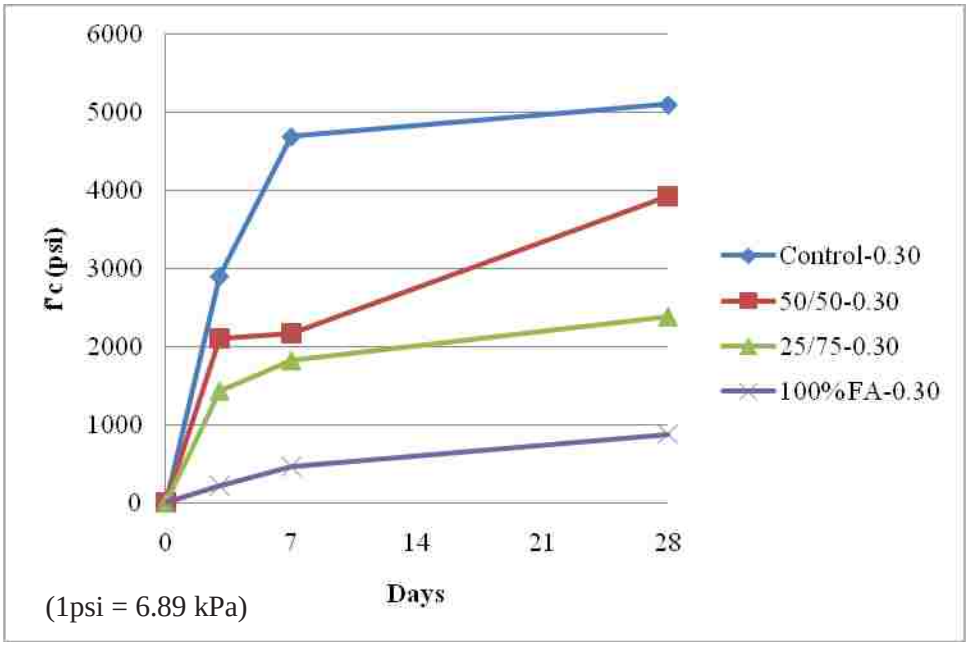

Figure C.2 - Mortar cube compressive strengths on test days (*w/cm* = 0.30)

Table C.6 – Compressive strengths for paste cubes

	Compressive Strength (psi)		
Specimen Set	**Day 1**	**Day 3**	**Day 7**
Control	1748	3919	5255
50/50	558	1920	3594
40/60	439	1571	2136
25/75	0	740	1266
100% FA	0	35	53
50/50-G	981	2500	3540
40/60-G	793	1701	2469
25/75-G	339	1271	1646
100% FA-G	0	0	71
50/50-G-10CH	1063	2529	2943
40/60-G-10CH	953	2243	2708
25/75-G-10CH	554	1219	1314
100% FA-G-10CH	671	670	748
50/50-G-15CH	1708	2649	3804
40/60-G-15CH	890	2390	3701
25/75-G-15CH	980	1075	1551
100% FA-G-15CH	624	616	580

(1 psi = 6.89 kPa)

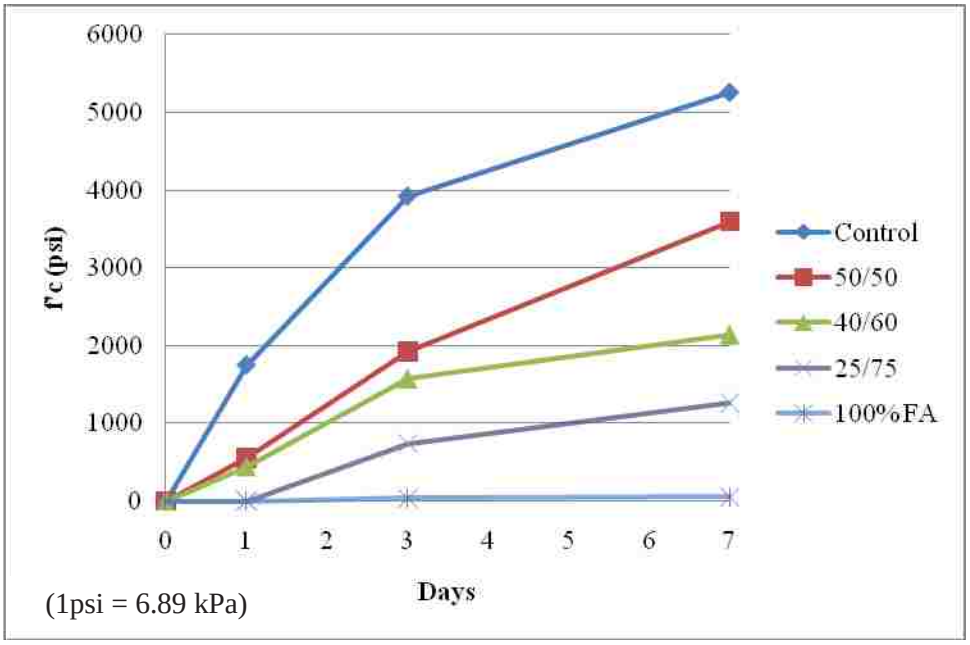

Figure C.3 – Paste cubes with no admixtures

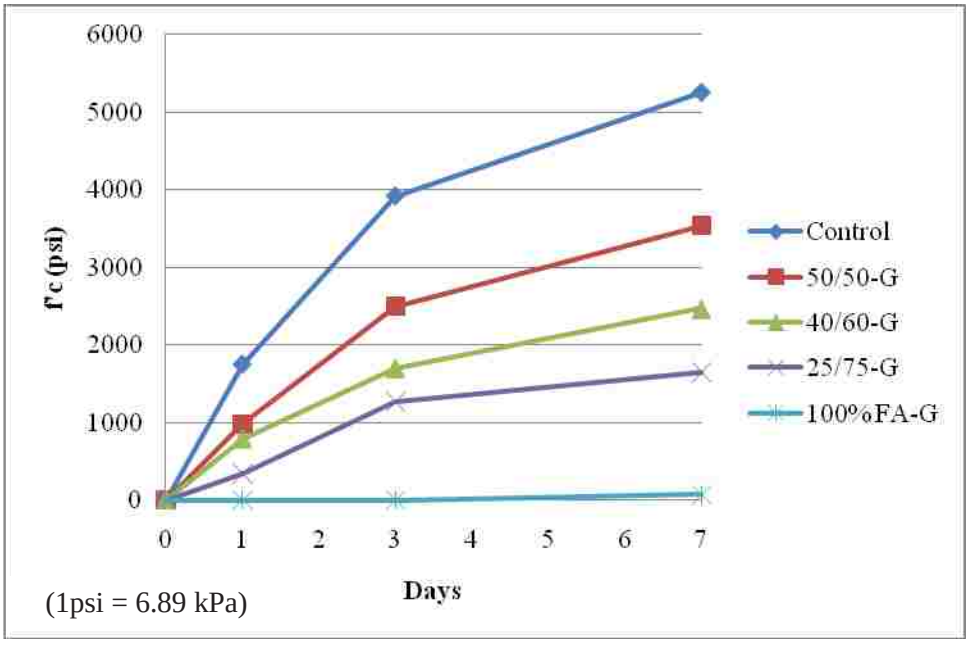

Figure C.4 – Paste Cubes with 4 percent gypsum

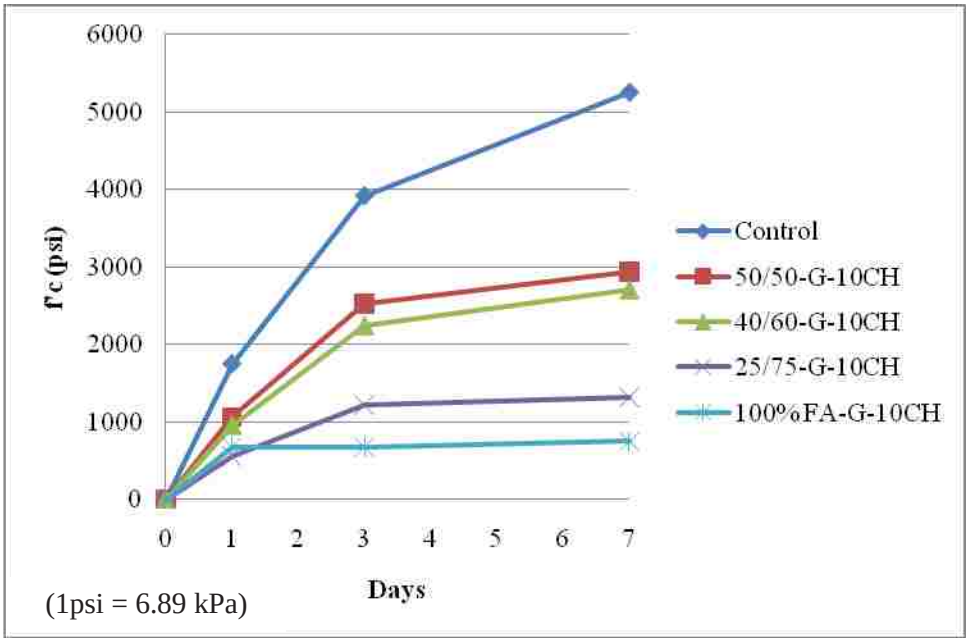

Figure C.5 – Paste Cubes with 4 percent gypsum and 10 percent calcium hydroxide

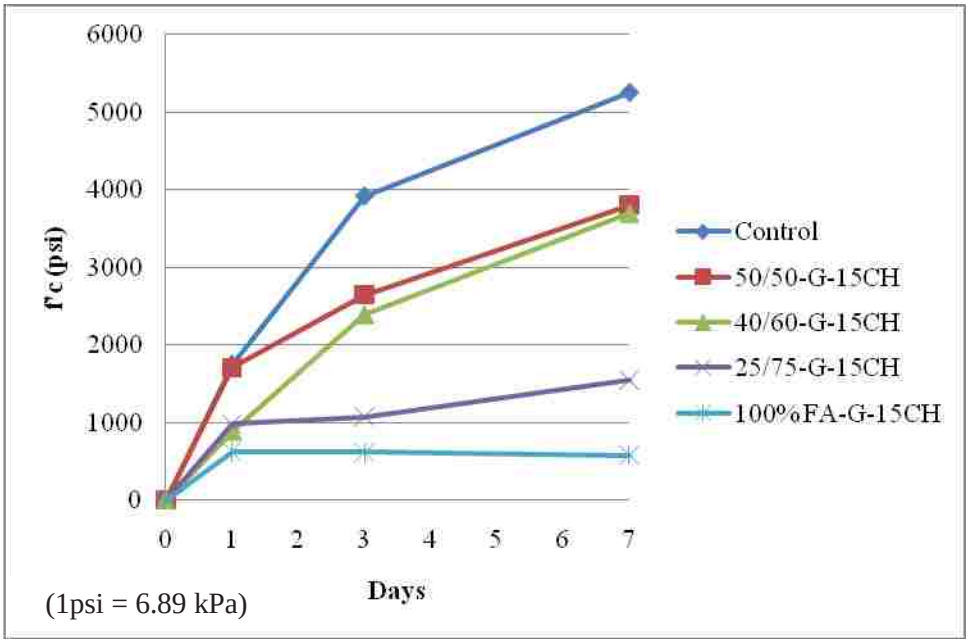

Figure C.6 – Paste Cubes with 4 percent gypsum and 15 percent calcium hydroxide

Table C.7 – Conventional mix description

Ingredient	Amount (lb/ft^3)
Water (Adjusted)	282.4
Portland cement	755.6
Coarse aggregate	1754.0
Fine aggregate	1110.5
w/c	0.45

(lb/ft^3 = 157 N/m^3)

Table C.8 – HVFA mix description

Ingredient		Amount (lb/ft^3)
Water (Adjusted)		282.4
Cementitious materials	Portland cement	230.0
	Fly ash	536.7
	Calcium hydroxide	59.5
	Gypsum	23.8
Coarse aggregate		1754.0
Fine aggregate		1016.0
w/cm		0.40

(lb/ft^3 = 157 N/m^3)

Table C.9 – Test Matrix for cylinder compression tests

		Cementitious Materials (%)			
Specimen Set *	w/cm	Fly Ash	Cement	Gypsum	CH
Control	0.45	0	100	4	10
HVFA (50%)	0.40	50	50	4	10
HVFA (60%)	0.40	60	40	4	10
HVFA (70%)	0.40	70	30	4	10
HVFA (75%)	0.40	75	25	4	10

*Each set is comprised of the average of three specimens

Table C.10 – Test results from cylinder compression tests

		Compressive Strength (psi)			
Specimen Set *	**w/c**	**Day 1**	**Day 3**	**Day 7**	**Day 28**
Control	0.40	3092	4537	5176	6188
HVFA (50%)	0.40	1189	2464	3982	5360
HVFA (60%)	0.40	1236	2671	3987	5475
HVFA (70%)	0.40	1121	1849	2877	4428
HVFA (75%)	0.40	657	1228	2002	3021

*Each set is comprised of the average of three specimens
(1 psi = 6.89 kPa)

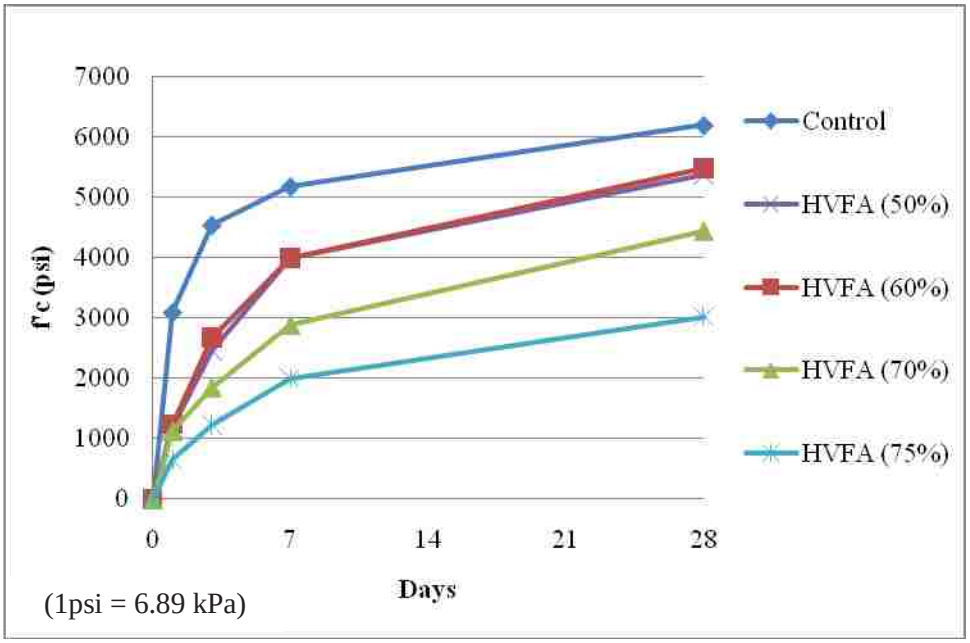

Figure C.7 – Compressive strength vs. test day plot for all cylinder mixes

Table C.11 – Tensile Test Data

Specimen	Peak Load (kips)	Yield Strength (ksi)	Yield Strain (in/in)
1	41402	72	0.0026
2	42157	78	0.0024
3	41983	77	0.0026
4	47228	68	0.0020
5	46890.8	68	0.0020
6	47106	68	0.0020
Average	44461	72	0.0023

(1 kip = 4.45 kN, 1 ksi = 6.89 MPa, 1 in = 25.4 mm)

APPENDIX D

STATISTICAL ANALYSIS

Table D.1 – t-test for CPO_4 and FAPO_4 specimen average comparisons

	Variable 1	*Variable 2*
Mean	155.684406	166.5778
Variance	15.80600925	10.64479
Observations	3	3
Pooled Variance	13.22539978	
Hypothesized Mean Difference	0	
df	4	
t Stat	-3.668626474	
P(T<=t) one-tail	0.010708505	
t Critical one-tail	2.131846782	
P(T<=t) two-tail	0.02141701	
t Critical two-tail	2.776445105	

Table D.2 – t-test for CPO_6 and FAPO_6 specimen average comparisons

	Variable 1	*Variable 2*
Mean	429.7987919	409.6753977
Variance	36.15162873	314.0897869
Observations	3	3
Pooled Variance	175.1207078	
Hypothesized Mean Difference	0	
df	4	
t Stat	1.862422083	
P(T<=t) one-tail	0.068009273	
t Critical one-tail	2.131846782	
P(T<=t) two-tail	0.136018546	
t Critical two-tail	2.776445105	

Table D.3 – t-test for Cont_NC and FA_NC specimen average comparisons

	Variable 1	*Variable 2*
Mean	321.3033762	351.6036816
Variance	61.73513886	261.355324
Observations	3	3
Pooled Variance	161.5452314	
Hypothesized Mean Difference	0	
df	4	
t Stat	-2.919749313	
P(T<=t) one-tail	0.021627151	
t Critical one-tail	2.131846782	
P(T<=t) two-tail	0.043254302	
t Critical two-tail	2.776445105	

Table D.4 – t-test for Cont_C and FA_C specimen average comparisons

	Variable 1	*Variable 2*
Mean	341.5993337	387.2061547
Variance	359.4000764	519.9382111
Observations	3	3
Pooled Variance	439.6691438	
Hypothesized Mean Difference	0	
df	4	
t Stat	-2.663866381	
P(T<=t) one-tail	0.028081794	
t Critical one-tail	2.131846782	
P(T<=t) two-tail	0.056163587	
t Critical two-tail	2.776445105	

BIBLIOGRAPHY

ACI 232R (2003). Use of Fly Ash in Concrete. *American Concrete Institute*, Farminton Hills, MI.

ACI 318 (2008). Building Code Requirements for Structural Concrete (ACI 318-08) and Commentary. *American Concrete Institute*, Farminton Hills, MI.

ACI 408R (2003). Bond and Development of Straight Reinforcing Bars in Tension. *American Concrete Institute*, Farminton Hills, MI.

ACI 211.1 (1991). Standard Practice for Selecting Proportions for Normal, Heavyweight, and Mass Concrete. *American Concrete Institute*, Farminton Hills, MI.

ASTM A 370 (2009). Standard Test Methods and Definitions for Mechanical Testing of Steel Products. *American Society for Testing and Materials*. West Conshohocken, PA.

ASTM C 109 (2008). Standard Test Method for Compressive Strength of Hydraulic Cement Mortars (Using 2-in. or [50-mm] Cube Specimens). *American Society for Testing and Materials*. West Conshohocken, PA.

ASTM C 143 (2010). Standard Test Methods for Slump of Hydraulic Cement Concrete. *American Society for Testing and Materials*. West Conshohocken, PA.

ASTM C 172 (2008). Standard Practice for Sampling Freshly Mixed Concrete. *American Society for Testing and Materials.* West Conshohocken, PA.

ASTM C 192 (2007). Standard Practice for Making and Curing Concrete Test Specimens in the Laboratory. *American Society for Testing and Materials*. West Conshohocken, PA.

ASTM C 231 (2009). Standard Test Method for Air Content of Freshly Mixed Concrete by the Pressure Method. *American Society for Testing and Materials*. West Conshohocken, PA.

ASTM C 31 (2009). Standard Practice for Making and Curing Concrete Test Specimens in the Field. *American Society for Testing and Materials*. West Conshohocken, PA.

ASTM C 39 (2009). Standard Test Method for Compressive Strength of Cylindrical Concrete Specimens. *American Society for Testing and Materials*. West Conshohocken, PA.

ASTM C 566 (1997). Standard Test Method for Total Evaporable Moisture Content of Aggregate by Drying. *American Society for Testing and Materials*. West Conshohocken, PA.

ASTM C 617 (2009). Standard Practice for Capping Cylindrical Concrete Specimens. *American Society for Testing and Materials*. West Conshohocken, PA 2009.

ASTM C 618 (2008). Standard Specification for Coal Fly Ash and Raw or Calcined Natural Pozzolan for Use in Concrete. *American Society for Testing and Materials*. West Conshohocken, PA.

ASTM C 618 (2008). Standard Specification for Coal Fly Ash and Raw or Calcined Natural Pozzolan for Use in Concrete. *American Society for Testing and Materials*. West Conshohocken, PA.

ASTM E 8 (2009). Standard Test Methods for Tension Testing of Metallic Materials. *American Society for Testing and Materials*. West Conshohocken, PA.

Bargaheiser, K., and Bualia, T. S., "Prevention of Corrosion in Concrete Using Fly Ash Concrete Mixes."

Bentz, D. P. and Ferraris, C. F. (2009). "Rheology and Setting of High Volume Fly Ash Mixtures." National Institute of Standards and Technology, Gaithersburg, MD.

Berry, M., Cross, D., Stevens, J. (2009). "Changing the Environment: An Alternative 'Green' Concrete Produced without Portland Cement." Montana State University, Bozeman, MT.

Cross, D., Stephens, J., and Vollmer, J. (n.d.). "Structural Applications of 100 Percent Fly Ash Concrete." Montana State University, Bozeman, MT.

Gopalakrishnan, S. (2005). "Demonstration of Utilising High Volume Fly Ash Based Concrete for Structural Applications." Structural Engineering Research Centre, Chennai India.

Hanle, L. J., Jayaraman, K. R., Smith, J.S. (2004). "CO_2 Emissions Profile of the U.S. Cement Industry." U.S. Environmental Protection Agency, Washington DC.

Headwaters Resources (2011). Fly Ash for Concrete. <http://www.flyash.com/data/upimages/press/fly%20ash%20for%20concrete.pdf>

Marlay, K. (2011). "Hardened Concrete Properties and Durability Assessment of High-Volume Fly Ash Concrete." Thesis. Missouri S&T, Rolla, MO.

Mindess, S., Young, F., Darwin, D. (2003) . *Concrete*. Prentice-Hall (2nd Edition).

Morotta, T. W. (2005). *Basic Construction Materials*. Prentice-Hall (7th Edition).

Naik, T.R., Singh, S. S., Sivasundaram, V. (1989). "Concrete Compressives Strength, Shrinkage and Bond Strength As Affected by Addition of Fly Ash and Temperature." The University of Wisconsin – Milwaukee, Milwaukee, WI.

Ramirez, J. A., and Russell, B. W. (2008). "Transfer, Development, and Splice Length for Strand/Reinforcement in High-Strength Concrete." *Report No. 603.* National Cooperative Highway Research Program, Washington, D.C.

RILEM 7-II-28. (1994). "Bond Test for Reinforcing Steel. 2. Pull-Out Test." E & FN Spon, London.

Swenty (2003). "Contamination Effects on the Bond Strength of Reinforcing Bars under Pullout Tests." Thesis. University of Missouri – Rolla, Rolla, MO.

U.S. Department of Transportation (2011). Coal Fly Ash – Material Description. <http://www.fhwa.dot.gov/publications/research/infrastructure/pavements/97148/016.cfm>

Zuo, J., Darwin, D. (2001). Splice Strength of Conventional and high Relative Rib Area Bars in Normal and high-Strength Concrete. *ACI Structural Journal,* 97-S65.

VITA

Michael Hayse Wolfe was born in West Lafeyette, Indiana. Michael grew up in Clinton, Mississippi and later graduated from Clinton High School in May 2005. Later that same year, he attended the University of Missouri-Rolla where he graduated with a Bachelor of Science degree in Civil Engineering in May 2009. Currently, Michael is attending the Missouri University of Science and Technology where he is working towards a Master of Science degree in Civil Engineering with a Structural emphasis with an expected graduation date of August 2011.